AMERICAN SOCIETY FOR MICROBIOLOGY | mBio

Check for updates

| Bacteriology | Research Article

Metabolic remodeling by RNA polymerase gene mutations is associated with reduced β-lactam susceptibility in oxacillin-susceptible MRSA

Shinya Watanabe,[1] Chijioke A. Nsofor,[1,2] Kanate Thitiananpakorn,[1] Xin-Ee Tan,[1] Yoshifumi Aiba,[1] Remi Takenouchi,[3] Kotaro Kiga,[1,4] Teppei Sasahara,[1] Kazuhiko Miyanaga,[1] Srivani Veeranarayanan,[1] Yuzuki Shimamori,[1] Adeline Yeo Syin Lian,[1] Thuy Minh Nguyen,[1] Huong Minh Nguyen,[1] Ola Alessa,[1] Geoffrey Peterkins Kumwenda,[1] Sarangi Jayathilake,[1] Jastin Edrian Cocuangco Revilleza,[1] Priyanka Baranwal,[1] Yutaro Nishikawa,[1] Feng-Yu Li,[1] Tomofumi Kawaguchi,[1] Sowmiya Sankaranarayanan,[1] Mahmoud Arbaah,[1] Yuancheng Zhang,[1] Maniruzzaman ,[1] Yi Liu,[1] Hossain Sarah,[1] Junjie Li,[1] Takashi Sugano,[1] Thi My Duyen Ho,[1] Anujin Batbold,[1] Tergel Nayanjin,[1] Longzhu Cui[1]

AUTHOR AFFILIATIONS See affiliation list on p. 18.

ABSTRACT The emergence of oxacillin-susceptible methicillin-resistant *Staphylococcus aureus* (OS-MRSA) has imposed further challenges to the clinical management of MRSA infections. When exposed to β-lactam antibiotics, these strains can easily acquire reduced β-lactam susceptibility through chromosomal mutations, including those in RNA polymerase (RNAP) genes such as *rpoBC*, which may then lead to treatment failure. Despite the increasing prevalence of such strains and the apparent challenges they pose for diagnosis and treatment, there is limited information available on the actual mechanisms underlying such chromosomal mutation-related transitions to reduced β-lactam susceptibility, as it does not directly associate with the expression of *mecA*. This study investigated the cellular physiology and metabolism of six missense mutants with reduced oxacillin susceptibility, each carrying respective mutations on RpoB^{H929P}, RpoB^{Q645H}, RpoC^{G950R}, RpoC^{G498D}, RpiA^{A64E}, and FruB^{A211E}, using capillary electrophoresis-mass spectrometry-based metabolomics analysis. Our results showed that *rpoBC* mutations caused RNAP transcription dysfunction, leading to an intracellular accumulation of ribonucleotides. These mutations also led to the accumulation of UDP-Glc/Gal and UDP-GlcNAc, which are precursors of UTP-associated peptidoglycan and wall teichoic acid. Excessive amounts of building blocks then contributed to the cell wall thickening of mutant strains, as observed in transmission electron microscopy, and ultimately resulted in decreased susceptibility to β-lactam in OS-MRSA.

IMPORTANCE The emergence of oxacillin-susceptible methicillin-resistant *Staphylococcus aureus* (OS-MRSA) strains has created new challenges for treating MRSA infections. These strains can become resistant to β-lactam antibiotics through chromosomal mutations, including those in the RNA polymerase (RNAP) genes such as *rpoBC*, leading to treatment failure. This study investigated the mechanisms underlying reduced β-lactam susceptibility in four *rpoBC* mutants of OS-MRSA. The results showed that *rpoBC* mutations caused RNAP transcription dysfunction, leading to an intracellular accumulation of ribonucleotides and precursors of peptidoglycan as well as wall teichoic acid. This, in turn, caused thickening of the cell wall and ultimately resulted in decreased susceptibility to β-lactam in OS-MRSA. These findings provide insights into the mechanisms of antibiotic resistance in OS-MRSA and highlight the importance of continued research in developing effective treatments to combat antibiotic resistance.

Invited Editor Poonam Mudgil, Western Sydney University, Penrith, New South Wales, Australia

Editor Gerald B. Pier, Harvard Medical School, Boston, Massachusetts, USA

Address correspondence to Shinya Watanabe, swatanabe@jichi.ac.jp.

The authors declare no conflict of interest.

See the funding table on p. 18.

Received 1 February 2024
Accepted 27 March 2024
Published 2 May 2024

KEYWORDS *Staphylococcus aureus*, MRSA, antimicrobial resistant, beta-lactams, OS-MRSA, oxacillin, RNA polymerases, rpoBC

Methicillin-resistant *Staphylococcus aureus* (MRSA) is one of the most distributed antibiotic-resistant bacterial pathogens in clinical settings, posing a significant threat to human health around the world (1). The breakpoints for diagnosing MRSA in clinical microbiology laboratories are defined as an oxacillin minimum inhibitory concentration (MIC) ≥ 4 µg/mL (Clinical and Laboratory Standards Institute) or cefoxitin MIC ≥ 8 µg/mL (European Committee on Antimicrobial Susceptibility Testing). β-Lactam resistance in MRSA is commonly associated with the expression of penicillin-binding protein 2a (PBP2a; also known as PBP2′), a peptidoglycan transpeptidase with low affinity for β-lactam antibiotics (2–4). Although β-lactam resistance is primarily mediated by the *mecA* gene encoding PBP2a, clinical MRSA isolates usually exhibit varying levels of β-lactam resistance, the diversity of which cannot be simply explained by the expression of PBP2a and the presence of functional *mecA* and *bla* regulators (MecI/MecR1/MecR2 and BlaI/BlaR1) (5–8). Oxacillin-susceptible MRSA (OS-MRSA) and borderline oxacillin-resistant *S. aureus* strains, both carrying *mecA* gene but exhibiting susceptible or borderline resistance to oxacillin, have been isolated in clinical settings (8–15). Owing to their susceptibility to oxacillin, OS-MRSA might be misidentified as methicillin-susceptible *S. aureus* (MSSA) by routine diagnostic tests in most clinical microbiology laboratories where *mecA* and PBP2a detections are unavailable. These oxacillin-susceptible MRSA strains readily express high-level resistance (homogeneous resistance phenotype) following exposure to β-lactams due to the presence of the *mecA* gene, similar to clinical isolates with a low-level β-lactam resistance phenotype, which are frequently reported to show heterogeneous expression of methicillin resistance due to the presence of a small proportion of resistant bacteria among the populations sensitive to β-lactams (16–19) and consequently cause treatment failure with β-lactam antibiotics that are commonly used to treat MSSA infections (20).

The transition from low- to high-level resistance is complex because the shift is often caused by gene mutations or genetic rearrangements that are not directly relevant to the function of *mecA* (8, 18, 21–29). Among the genes responsible for β-lactam resistance, RNA polymerase (RNAP) genes, *rpoBC,* are frequently found mutated in laboratory-derived β-lactam-resistant mutants (8, 21, 25). RNAP is a DNA-dependent RNA polymerase that catalyzes RNA synthesis in all cellular organisms (30). In Gram-positive bacteria, a RNAP holoenzyme consists of four essential (α2ββ′) and four accessory (δεσω) subunits (31). Since RNAP is the major central transcriptional machinery in bacterial cells, mutations in any of the RNAP subunits can affect cellular activities and antimicrobial susceptibility. Mutations in the *rpoA* gene, which encodes the α subunit of RNAP, have been reported to alter the promoter recognition domain and lead to a change in cellular phenotype (32). Mutations in the *rpoB* and *rpoC* genes decrease RNAP fidelity (33) and, as the binding site of rifampicin is located in the β subunit of RNAP at the DNA:RNA binding cleft, the mutations of *rpoB* gene paralleled a block in RNA extension and caused rifampicin resistance (34). In *Mycobacterium tuberculosis*, *rpoB* mutations caused rifampicin resistance while increasing cell wall permeability and susceptibility toward vancomycin (35). Other than conferring β-lactam and rifampicin resistance, *rpoBC* mutations contributed to vancomycin resistance, autolysis activity, and slow growth in MRSA (36–39). Importantly, MRSA strains carrying *rpoB* mutations have been isolated from patients who underwent long-term antibacterial treatment, and the isolates were shown to be expressing increased β-lactam resistance (40, 41). Despite the extensive reports on the association between RNAP mutations and antimicrobial susceptibility, the molecular mechanisms of β-lactam resistance mediated by *rpoBC* mutations have not been fully understood.

Recently, we collected 43 genetically diverse clinical OS-MRSA strains, which could be classified into 11 MLST types and 4 different SCC*mec* types (8). Mutations associated with oxacillin susceptibility were identified by analyzing the whole genome of 100

mutants with reduced oxacillin susceptibility derived from 26 representative OS-MRSA strains of seven main phylogenetic clades (8). Among these mutants, *rpoBC* genes were found to be most frequently mutated regardless of the varied genetic backgrounds in the parent strains. Interestingly, we also found that the expression of *mecA* and PBP2a was not significantly correlated with the oxacillin MICs of these OS-MRSA-derived mutants, although the *mecA* gene is essential for high-level β-lactam resistance because *mecA* deletion in RpoC^{P358L}, RpoB^{G645H}, and RpoC^{G498D} mutants showed a decrease in oxacillin MIC from 4, 32, and 256 µg/mL, respectively, to 0.38 µg/mL, a level similar to that of *mecA*-knockout mutant JMUB217(Δ*mecA*) (8). These findings emphasized the need for further investigation into the mechanisms underlying reduced oxacillin susceptibility in these mutants. In our present study, we aimed to unravel the mechanism associated with *rpoBC*-mediated acquisition of β-lactam resistance by investigating the cellular metabolisms of OS-MRSA-derived mutants with reduced oxacillin susceptibility. We focused on ribonucleotide metabolisms due to a clear downregulation of purine/pyrimidine biosynthesis and nucleotide transporter genes (*xprT*, *purF*, *guaAB*, *pyrRP*, and *hisIG*) observed in the transcriptome analysis of the representative *rpoBC* mutants with reduced oxacillin susceptibility (8).

RESULTS

Antibiotic susceptibility of mutants with reduced oxacillin susceptibility

Chromosomal mutations responsible for reduced oxacillin susceptibility in mutant strains derived from OS-MRSA were previously identified (8). These mutations were found to be distributed among 46 genes classified into various functional categories. To gain more insight into the molecular mechanisms regulating the decrease of β-lactam susceptibility in OS-MRSA, six representative mutants with reduced oxacillin susceptibility derived from the JMUB217 strain were further analyzed (8). JMUB217-7 (RpiA^{A64E}), JMUB217-13 (FruB^{A211E}), JMUB217-23 (RpoB^{H929P}), JMUB217-22 (RpoB^{Q645H}), JMUB217-19 (RpoC^{G950R}), and JMUB217-24 (RpoC^{G498D}) are included in this study because (i) single mutation was detected on their chromosomes, and (ii) RNAP genes (*rpoBC*), purine biosynthesis gene (e.g., *rpiA*), and glycolysis gene (e.g., *fruB*) were the most frequently mutated genes identified among mutants with reduced oxacillin susceptibility in our previous study (8). In addition, three mutation-repaired strains of JMUB217-7 (RpiA^{A64E}), JMUB217-22 (RpoB^{Q645H}), and JMUB217-24 (RpoC^{G498D}) were constructed. MICs of eight antibiotic agents for all the JMUB217-derived mutants and mutation-repaired strains were determined. As described previously, the oxacillin MIC increased from 1.0 ± 0.0 µg/mL in wild-type strain to 3.0 ± 0.0, 11 ± 2.3, 43 ± 9.2, 171 ± 74, 21 ± 4.6, and 64 ± 0.0 µg/mL in JMUB217-7, JMUB217-13, JMUB217-23, JMUB217-22, JMUB217-19, and JMUB217-24, respectively (Fig. 1). Similar to oxacillin, the JMUB217-derived mutants exhibited increment in MIC of other β-lactam antibiotics, including cefoxitin and imipenem (Fig. 1), while their susceptibility against other cell wall synthesis inhibitors, such as vancomycin, teicoplanin, and fosfomycin, did not differ from wild-type JMUB217. On the other hand, the three mutation-repaired strains showed similar levels of MICs to the wild-type strains. We have also determined the rifampicin MIC of the mutants because it has been reported that mutations in *rpoB* increased rifampicin MIC (42, 43). However, all mutants with reduced oxacillin susceptibility were susceptible to rifampicin (Fig. 1).

mecA and purine biosynthesis gene expressions of mutants with reduced oxacillin susceptibility

Expression of *mecA* and key enzymes of the purine biosynthesis pathway, *purF* and *guaA,* was determined by qRT-PCR (Fig. 2) to confirm our previous findings (8). *mecA* expression profiles of the six representative mutants with reduced oxacillin susceptibility and the three mutation-repaired strains were studied, with MRSA strains COL (ST256, SCC*mec* type I, oxacillin MIC > 256 µg/mL) and USA300_C02 (ST8, SCC*mec* type IVa,

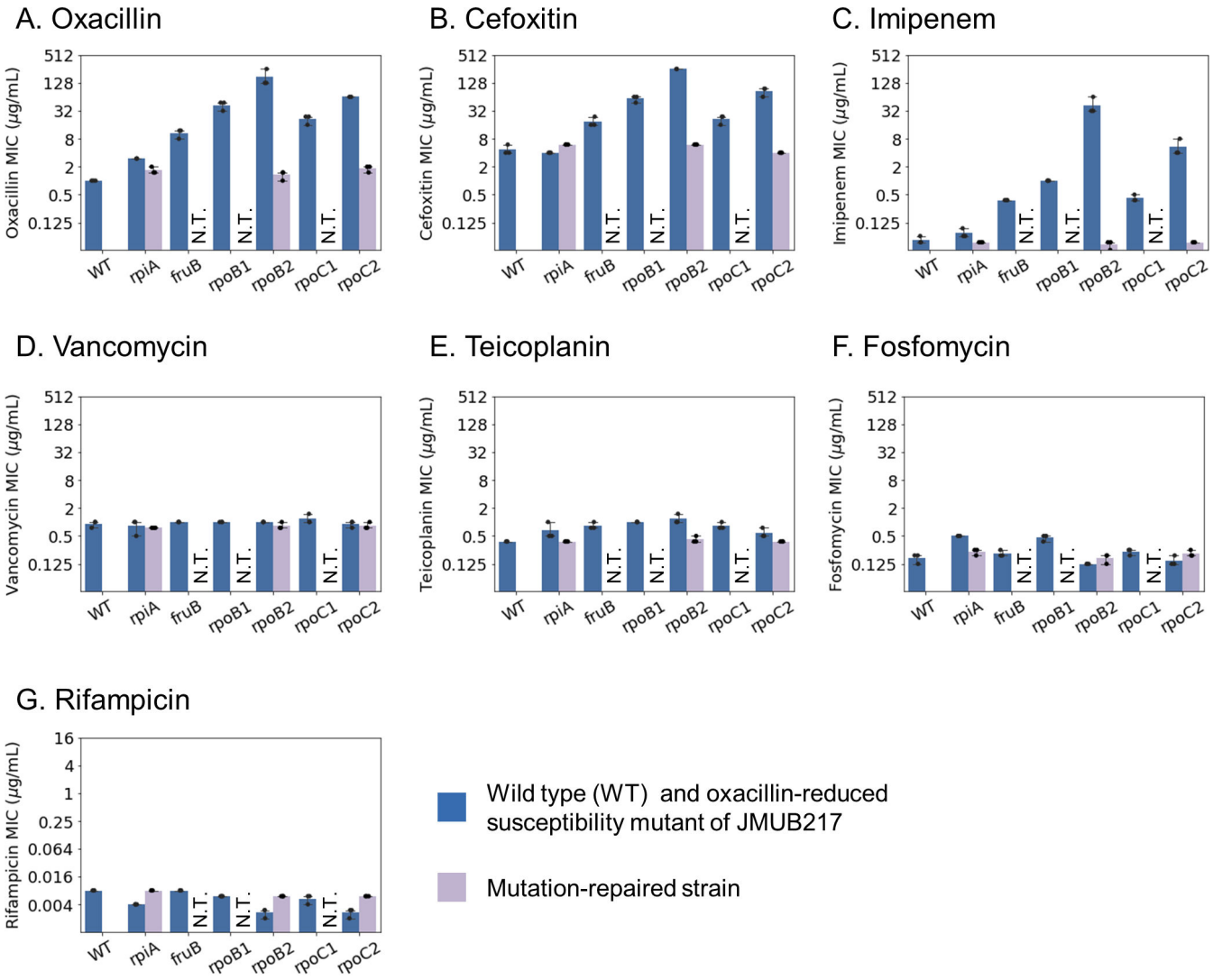

FIG 1 MIC of the JMUB217-derived mutants. MICs of eight drugs for six JMUB217-derived mutants with reduced oxacillin susceptibility: *rpiA* (JMUB217-7 RpiA^{A64E}), *fruB* (JMUB217-13 FruB^{A211E}), *rpoB1* (JMUB217-23 RpoB^{H929P}), *rpoB2* (JMUB217-22 RpoB^{Q645H}), *rpoC1* (JMUB217-19 RpoC^{G950R}), and *rpoC2* (JMUB217-24 RpoC^{G498D}) and mutation-repaired strains of JMUB217-7 (*rpiA*), JMUB217-22 (*rpoB2*), and JMUB217-24 (*rpoC2*) were determined. MICs were measured using E-test, and the graph represents the mean ± SD of biological triplicates.

oxacillin MIC of 48 µg/mL) included in the analysis as MRSA reference strains. Our results showed that *mecA* expressions were not significantly increased in the six mutant strains, with or without oxacillin induction, compared with COL and USA300_C02 (Fig. 2A), indicating that their basal and induced *mecA* expression levels were lower than those of MRSA. On the other hand, both *purF* and *guaA* expressions, which were significantly downregulated in JMUB217-22 (RpoB^{Q645H}), JMUB217-19 (RpoC^{G950R}), and JMUB217-24 (RpoC^{G498D}) (Fig. 2C and D), were rescued in the mutation-repaired strains of JMUB217-22 and JMUB217-24. These results indicated that the *rpoBC* mutations are mediating downregulations of the purine biosynthesis pathway, comparable to RNA-seq analysis in our previous study.

Metabolic remodeling through oxacillin-induced mutations

Untargeted metabolomics was applied to study metabolic changes in the OS-MRSA strain JMUB217 and its six derivative mutants with reduced oxacillin susceptibility. Three biological replicates were prepared from the mid-log phase culture, and all samples were

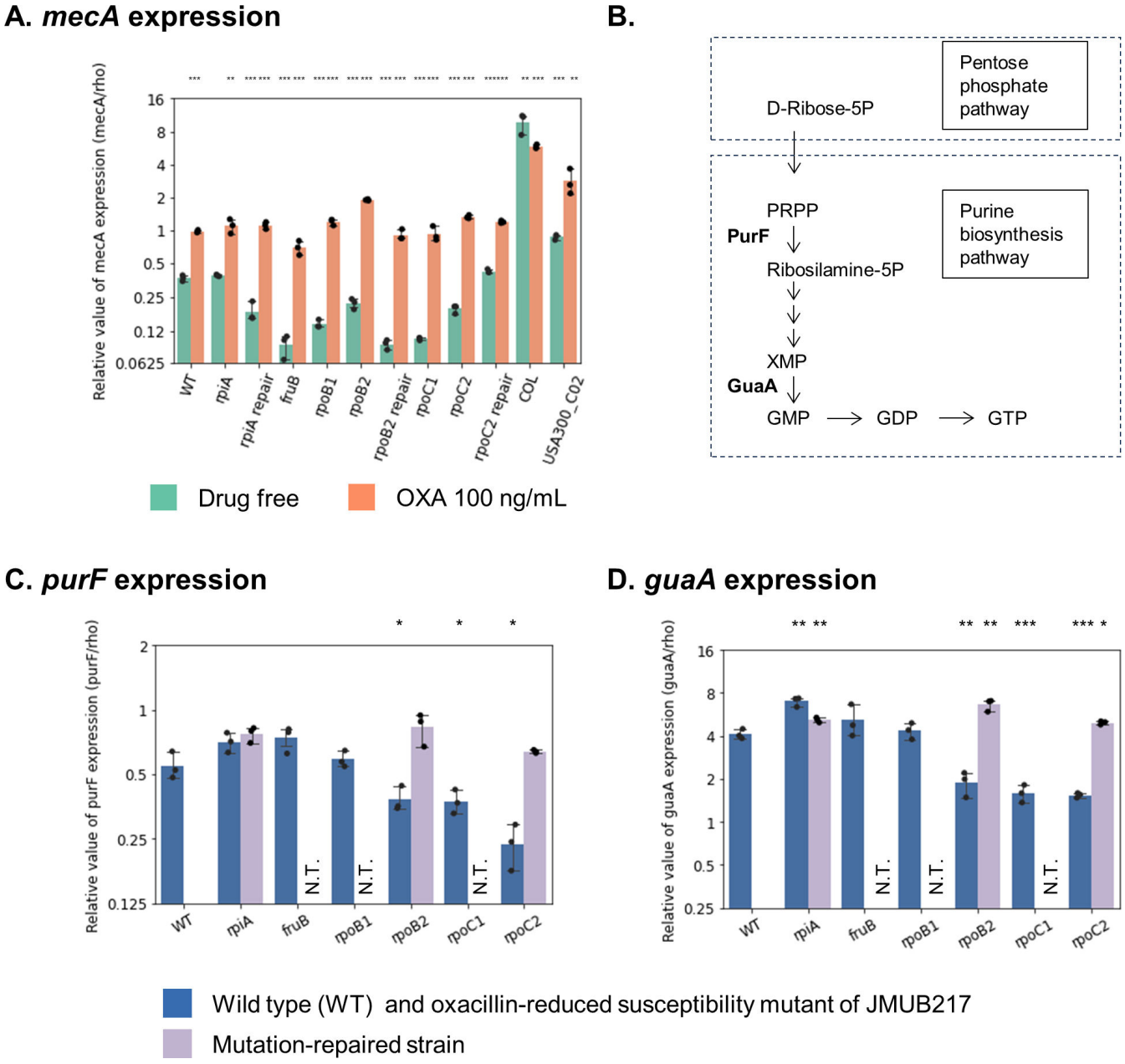

FIG 2 RNA expression levels of JMUB217-derived mutants. qRT-PCR results for (A) *mecA*, (C) *purF*, and (D) *guaA* in six JMUB217-derived mutants with reduced oxacillin susceptibility: *rpiA* (JMUB217-7 RpiA^{A64E}), *fruB* (JMUB217-13 FruB^{A211E}), *rpoB1* (JMUB217-23 RpoB^{H929P}), *rpoB2* (JMUB217-22 RpoB^{Q645H}), *rpoC1* (JMUB217-19 RpoC^{G950R}), and *rpoC2* (JMUB217-24 RpoC^{G498D}); three mutation-repaired strains (*rpiA*, *rpoB2,* and *rpoC2*); and two reference MRSA strains COL and USA300_C02 with or without exposure to 100 ng/mL oxacillin. The data are shown as means ± SD of three biological replicates. *, **, ***, and ns indicate $P < 0.05$, 0.01, 0.001, and not significant, respectively, given by the Student's *t*-test. (B) Purine biosynthesis pathway of *S. aureus* JMUB217.

analyzed using the capillary electrophoresis time-of-flight mass spectrometry (CE-TOF-MS) for metabolomic profiling (44, 45). A total of 273 metabolite peaks (153 in cation and 120 in anion mode) were detected and annotated by the peak library (Fig. 3A). Detailed metabolomic profiles are presented in Table S1. Principal component analysis (PCA) of the metabolic data revealed clear clustering between mutated genes (Fig. 3B), with the first and second principal components (PC1 and PC2) accounting for 32.8% and 13.1% of the total variance, respectively. RNAP mutations were clearly correlated with PC1 because the metabolites of *rpoB* and *rpoC* mutated strains were positively aligned with PC1. Moreover, the PCA plots of the *rpoB* and *rpoC* groups partially overlapped with each

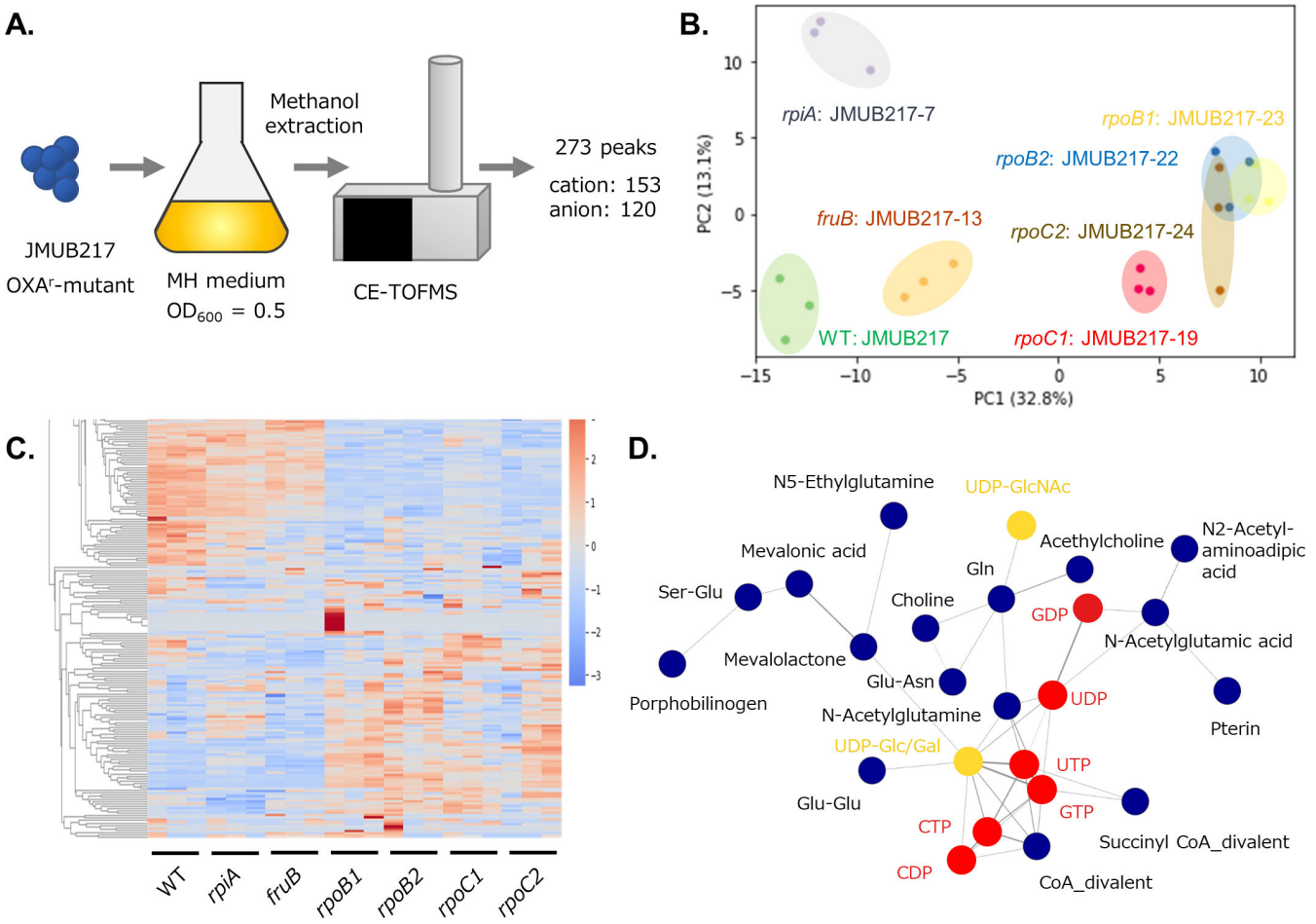

FIG 3 Metabolomic analysis of JMUB217-derived mutants. (A) Schematic diagram depicting the workflow of metabolomics analysis by CE-TOF-MS. (B) PCA score plot of metabolites in JMUB217-derived mutants with reduced oxacillin susceptibility: *rpiA* (JMUB217-7 RpiA^{A64E}), *fruB* (JMUB217-13 FruB^{A211E}), *rpoB1* (JMUB217-23 RpoB^{H929P}), *rpoB2* (JMUB217-22 RpoB^{Q645H}), *rpoC1* (JMUB217-19 RpoC^{G950R}), and *rpoC2* (JMUB217-24 RpoC^{G498D}). (C) Heat map representation of the metabolome analyzed by hierarchical clustering analysis. The distances between peaks are displayed in tree diagrams. Red and blue colors indicate higher and lower levels of metabolites, respectively. (D) Network analysis of the metabolites of JMUB217-derived mutants. Generally, metabolites are presented in blue circles, while ribonucleotides and their derivatives are highlighted in red and yellow, respectively. Figures 3 to 5 and Fig. S1 were constructed from data of the same metabolomics analysis.

other, indicating that the four different mutations in *rpoBC* affected the metabolism of *S. aureus* in a similar manner. This observation was supported by hierarchical clustering analysis of the metabolomics data, which showed a marked difference in the metabolic profiles between *rpoBC* mutants and wild-type or the other strains carrying *rpiA* and *fruB* mutations (Fig. 3C). The heat map has indeed identified a group of metabolites specifically accumulated in *rpiA*-mutated cells distinct from *rpoBC*- and *fruB*-mutated cells (Fig. 3C). To identify co-accumulated metabolites in *rpoBC*-mutated cells, network analysis was performed. The analysis revealed 15 clusters of co-accumulated metabolites in JMUB217 and its mutants with reduced oxacillin susceptibility. One of the clusters contains 24 metabolites, which were specifically accumulated in *rpoBC* mutants (Fig. 3D). The cluster includes (i) ribonucleoside-di/triphosphate (GDP, UDP, CDP, GTP, UTP, and CTP) and its derivatives (UDP-GlcNac, UDP-Glc/Gal); (ii) glutamine/glutamate and its derivatives (Gln, Ser-Glu, Glu-Glu, N-acetylglutamine, N-acetylglutamic acid, N5-ethylglutamine); and (iii) CoA/succinyl CoA divalents (Fig. 3D). Metabolomics profiling clearly demonstrated the accumulation of metabolites in a mutation-specific manner.

Ribonucleoside di/triphosphate accumulation resulted from *rpoBC* mutations

Network analysis of the metabolomics data revealed an accumulation of ribonucleoside di/triphosphate in the *rpoBC* mutants. The build-up of excess ribonucleoside di/triphosphate is consistent with the downregulation of purine/pyrimidine biosynthesis and nucleotide transporter genes observed through RNA-seq analysis of the *rpoBC* mutants (8). To obtain a comprehensive overview of nucleotide metabolisms in *rpoBC* mutants, the levels of intracellular ribonucleotide/deoxyribonucleotide in mutants with reduced oxacillin susceptibility are summarized in Fig. 4. Remarkably, GTP achieved 3.6-, 3.0-, 2.5-, and 2.9-fold greater accumulation in JMUB217-23 ($RpoB^{H929P}$), JMUB217-22 ($RpoB^{Q645H}$), JMUB217-19 ($RpoC^{G950R}$), and JMUB217-24 ($RpoC^{G498D}$), respectively (Fig. 4). CTP also exhibited a respective 6.2-, 7.5-, 3.6-, and 4.8-fold increase, while UTP showed 4.9-, 4.0-, 3.2-, and 3.8-fold increase in JMUB217-23, JMUB217-22, JMUB217-19, and JMUB217-24, respectively (Fig. 4). ATP was slightly accumulated in *rpoB* mutants but remained unaffected in *rpoC* mutants. On the contrary, intracellular ribonucleoside monophosphates, especially GMP and AMP, were reduced in the *rpoBC* mutants. In contrast to ribonucleotide, a modest intracellular accumulation of dGTP and dCTP was observed in the *rpoB* mutants, while most of the deoxyribonucleoside phosphates were either unchanged or decreased in the mutants with reduced oxacillin susceptibility. In short, the metabolomics results showed that *rpoBC* mutations stimulated intracellular ribonucleoside di/triphosphate accumulation in OS-MRSA.

Global metabolic alterations resulted from *rpoBC* mutations

The accumulation of ribonucleoside di/triphosphate is proposed to be a sequela of RNAP hypofunctioning caused by *rpoBC* mutations because ribonucleotides are building blocks of RNA (Fig. 5A). To elucidate the effect of *rpoBC* mutations on the transcription activity of RNAP, the total amount of RNA in mutants with reduced oxacillin susceptibility was measured. The mutations in *rpoBC* genes facilitated a substantial decrease in the levels of total RNA (Fig. 5B), whereby a respective 0.56-, 0.44-, 0.84-, and 0.76-fold decrease in total RNAs was observed in JMUB217-23, JMUB217-22, JMUB217-19, and JMUB217-24 (Fig. 5B). In addition, *rpiA* and *fruB* mutants also showed a slight decrease in total RNA. Thus, we deduced that *rpoBC* mutations reduced the general transcription activity of cells *in vivo*, thereby resulting in the accumulation of intracellular ribonucleoside di/triphosphate.

Nucleoside triphosphates (NTPs) are substrates of nucleoside diphosphate (NDP) sugars, which are important for the biosynthesis of many biological molecules, e.g., lipopolysaccharides, glycoproteins, and peptidoglycans. Therefore, excessive amounts of NTPs found in the *rpoBC* mutants are hypothesized to be consumed as NDP sugars and lead to peptidoglycan and lipoteichoic acid production (Fig. 5A). In this study, UDP-glucose/galactose (UDP-Glc/Gal; the two molecules could not be distinguished by CE-TOF-MS because they have the same molecular weight) and UDP-N-acetylglucosamine (UDP-GlcNAc) were measured by metabolomics analysis (Fig. 5C). As expected, intracellular UDP-Glc/Gal significantly increased in the *rpoBC* mutants, and UDP-GlcNAc (one of the important constituents of peptidoglycan) was significantly accumulated in JMUB217-23. In concordance with the accumulation of UDP-GlcNAc, three of the four amino acids, Gly, Lys, and Ala, required for peptidoglycan biosynthesis were significantly reduced in the *rpoBC* mutants, while their cellular levels of co-enzyme A divalent (CoA) were found to be increased.

To confirm that the accumulation of NTPs and UDP-carbohydrates are mediated by RNAP gene mutations, we re-extracted metabolites of three representative studied strains: wild-type JMUB217, JMUB217-22 (*rpoB2*), and its mutation-repaired derivative, and their differential metabolomics profiles were analyzed using CE-TOF-MS. Our results showed that the accumulation of GTP/CTP/UTP, UDP-Glu/Gal and UDP-GlcNac in the JMUB217-22 was recovered in its mutation-repaired derivative to a level similar to that of the wild-type JMUB217 (Fig. 6). The consumption of peptidoglycan precursors in

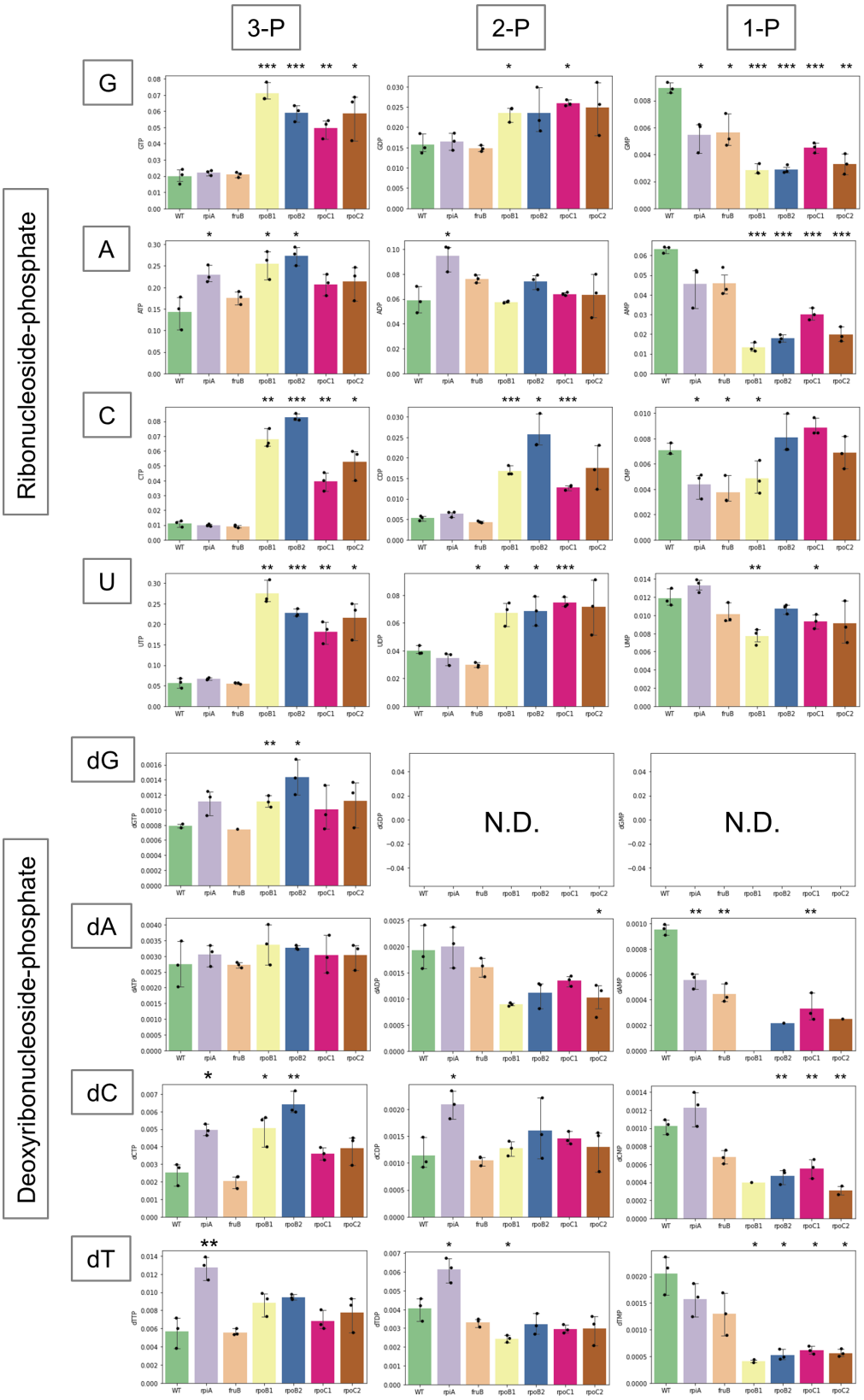

FIG 4 Ribo/deoxyribonucleotide profile of JMUB217-derived mutants. Quantitative values of each ribo/deoxyribonucleotide of JMUB217-derived mutants with reduced oxacillin susceptibility: *rpiA* (JMUB217-7 RpiA^{A64E}), *fruB* (JMUB217-13 FruB^{A211E}), *rpoB1* (JMUB217-23 RpoB^{H929P}), *rpoB2* (JMUB217-22 RpoB^{Q645H}), *rpoC1* (JMUB217-19 RpoC^{G950R}), and *rpoC2* (JMUB217-24

(Continued on next page)

FIG 4 (Continued)

RpoC^{G498D}). The *y*-axis represents the amount of intracellular ribo/deoxyribonucleotide (pmol) in 1 mL of cell suspension at OD_{600} = 1. Data represent means with standard error from three independent experiments. N.D., not detected. Mean values of intracellular ribo/deoxyribonucleotide of mutant strains were compared with that of wild-type via one-way ANOVA. *$P < 0.05$, **$P < 0.01$, and ***$P < 0.001$. Figures 3 to 5 and Fig. S1 were constructed from data of the same metabolomics analysis.

rpoBC mutants suggested that peptidoglycan biosynthesis in these cells could have been promoted.

Ribonucleoside di/triphosphate accumulation reduced oxacillin susceptibility of *rpoBC* mutants

To confirm the causal relationship between oxacillin susceptibility and the accumulation of ribonucleoside di/triphosphate, *rpoBC* mutants expressing cyclic UMP (cUMP) and cyclic CMP (cCMP) synthase were constructed, and their oxacillin MIC was determined. cUMP and cCMP synthases encoded in Pycsar (pyrimidine cyclase system for antiphage resistance) were known to consume intracellular UTP and CTP for the generation of cUMP and cCMP, respectively (46), affecting the intracellular ribonucleotide di/triphosphate pool. JMUB217 was found to carry the cUMP synthase gene on the chromosome, though the effector gene was disrupted by the insertion of IS, while the cCMP synthase gene was detected in another OS-MRSA strain, JMUB4998 (8). In this study, JMUB217-22 (*rpoB*) and JMUB217-24 (*rpoC*) were, respectively, transformed with aTc-inducible pLC1t2 plasmid containing JMUB217-derived cUMP and JMUB4998-derived cCMP synthase genes. aTc induction increased oxacillin susceptibility in both transformants, suggesting that intracellular UTP and CTP can affect the oxacillin susceptibility of *rpoBC* mutants. The slight increase in oxacillin susceptibility without aTc induction is probably due to promoter leakage (Fig. 7).

Metabolic alterations caused by *fruB* and *rpiA* mutations

FruB (1-phosphofructokinase) catalyzes the ATP-dependent phosphorylation of fructose-1-phosphate to fructose-1,6-bisphosphate (Fru-1,6P_2) (47). Therefore, it is expected that a mutation in the *fruB* gene will affect the intracellular level of these two metabolites. Our results showed that fructose/glucose-1P (Fru/Glc-1P), which could not be distinguished by CE-TOF-MS due to having the same molecular weight, was accumulated in the *fruB* mutant, while intracellular Fru-1,6P_2 was not affected by the *fruB* mutation (Fig. S1). We concluded that the FruB^{A211E} mutation is a loss-of-function mutation because of the intracellular accumulation of substrate Fru-1P. Most of the other metabolites were not altered by this mutation.

RpiA (ribose 5-phosphate isomerase A) is a key regulator of the pentose phosphate pathway, which catalyzes the conversion of D-ribose 5-phosphate to D-ribulose 5-phosphate (48). Similar to the case of the *fruB* mutation, the mutation of *rpiA* facilitated the accumulation of substrate ribulose-5P, while the product ribose-5P was not changed, indicating that the *rpiA* mutation induces loss of function (Fig. S1). However, in contrast to the *fruB* mutation, mutated *rpiA* broadly enhanced the accumulation of metabolites of the pentose phosphate and glycolysis pathways.

Cell wall thickening in the mutants with reduced oxacillin susceptibility

The cell wall thickness of the mutants with reduced oxacillin susceptibility was determined in order to investigate the effect of *rpoBC* mutations on peptidoglycan biosynthesis, as our previous studies have shown alterations in the profile of intracellular metabolites associated with this process. Wild-type OS-MRSA JMUB217 had a cell wall thickness of 22.07 ± 1.39 nm, while the mutants carrying *rpoBC* mutations with reduced oxacillin susceptibility had significantly thicker cell walls (Fig. 8). The mean cell wall thicknesses were 25.91 ± 1.99, 25.88 ± 1.99, 23.47 ± 3.15, and 28.48 ± 2.41 nm in JMUB217-23 (RpoB^{H929P}), JMUB217-22 (RpoB^{Q645H}), JMUB217-19 (RpoC^{G950R}),

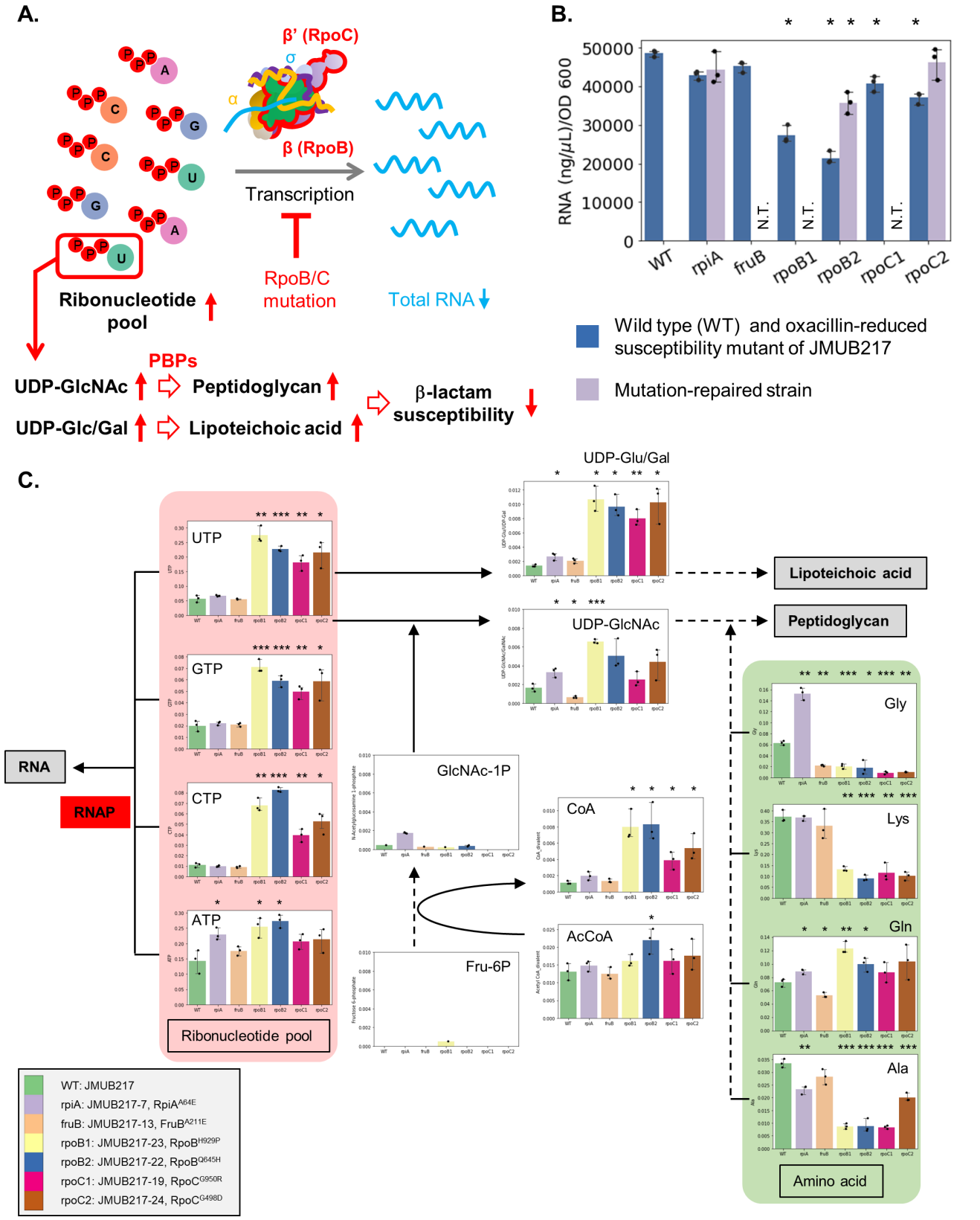

FIG 5 Metabolic alterations associated with *rpoBC* mutations. (A) Proposed mechanism of reduced β-lactam susceptibility mediated by *rpoBC* mutations. *rpoB/C* mutations cause dysregulation of RNAP transcription activity and a subsequent intracellular accumulation of ribonucleotides. Excessive accumulation of UTP enhances the production of UDP-GlcNAc and UDP-Glc/Gal, resulting in cell wall thickening and reduced β-lactam susceptibility in OS-MRSA. (B) The total amount

(Continued on next page)

FIG 5 (Continued)

of RNA in JMUB217-derived mutants grown to the mid-log phase (OD_{600} = 0.5). (C) RNA and peptidoglycan biosynthesis pathway of JMUB217-derived mutants. The *y*-axis represents the amount of intracellular metabolites (pmol) in 1 mL of cell suspension at OD_{600} = 1. Data represent means with standard error from three independent experiments. Mean values of intracellular metabolites of mutant strains were compared with that of wild-type via one-way ANOVA. **P* < 0.05, ***P* < 0.01, and ****P* < 0.001. Figures 3 to 5 and Fig. S1 were constructed from data of the same metabolomics analysis.

and JMUB217-24 ($RpoC^{G498D}$), respectively. Interestingly, the cell walls of *rpiA* and *fruB* mutants were also shown to be thickened (23.83 ± 2.31 and 23.32 ± 1.65 nm, respectively).

DISCUSSION

The emergence and spread of methicillin-resistant *Staphylococcus aureus* have become a major public health concern, as it can cause severe infections that are difficult to treat (1). OS-MRSA is a subtype of MRSA that is sensitive to oxacillin but still resistant to some β-lactam antibiotics (8–15). It has the potential to become highly resistant if exposed to β-lactam antibiotics, leading to treatment failure and further compounding the burden of diseases caused by *S. aureus*. Over decades, OS-MRSA have been isolated from various sources, including humans (both in the hospitals and community settings), animals,

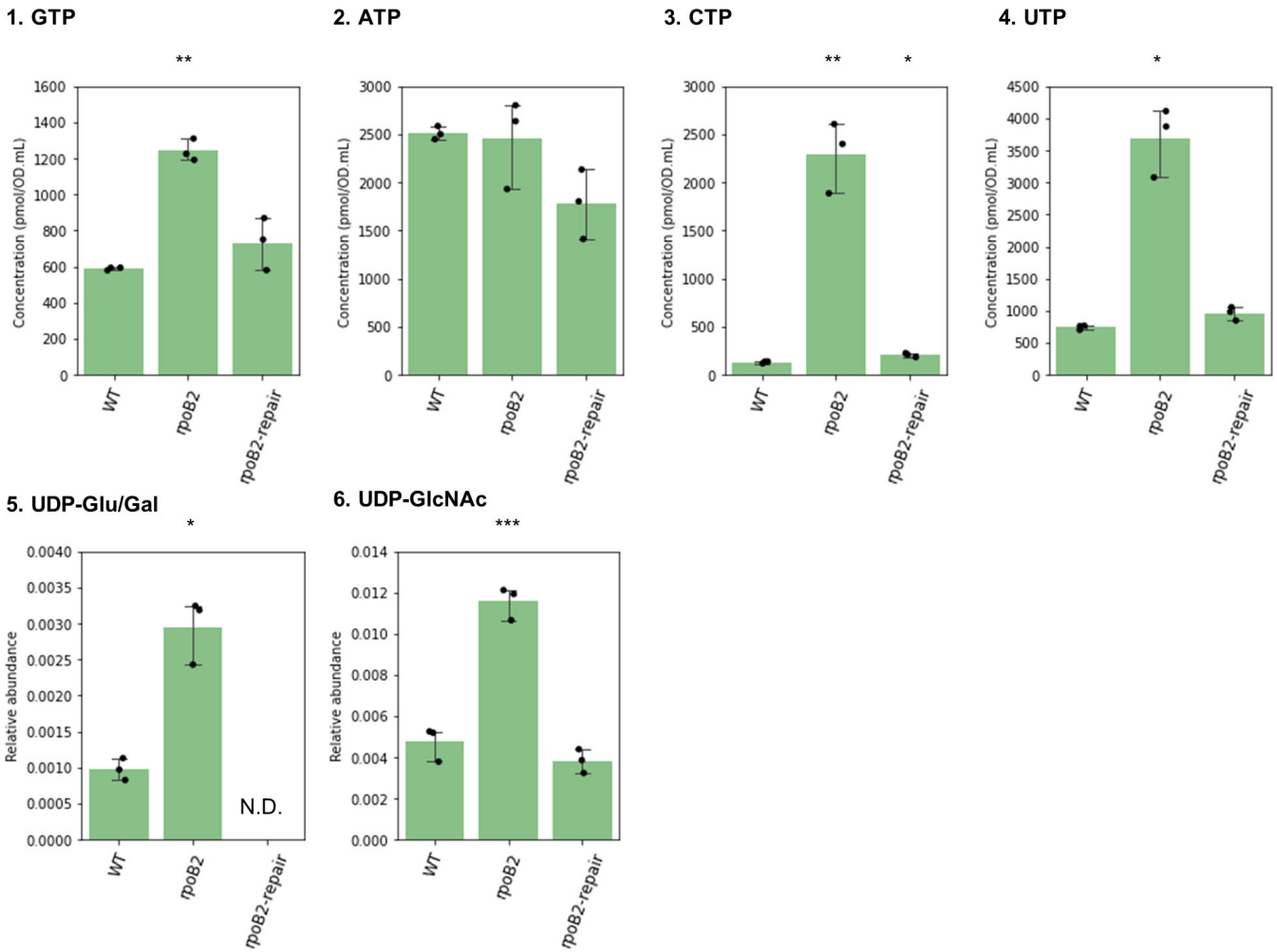

FIG 6 Intracellular levels of nucleoside triphosphates and UDP-carbohydrate of *rpoB* mutant and its mutation-repaired strain. Relative values of GTP, ATP, CTP, and UTP, and relative abundances of UDP-Glu/Gal and UDP-GlcNAc of JMUB217-derived mutant (*rpoB2*) and its mutation-repaired strain (*rpoB2*-repair). Mean values of intracellular metabolites of mutant/mutation-repaired strains were compared with that of wild type via one-way ANOVA. **P* < 0.05, ***P* < 0.01, and ****P* < 0.001. Figure 6 was constructed using metabolomics data different from Fig. 3 to 5 and Fig. S1.

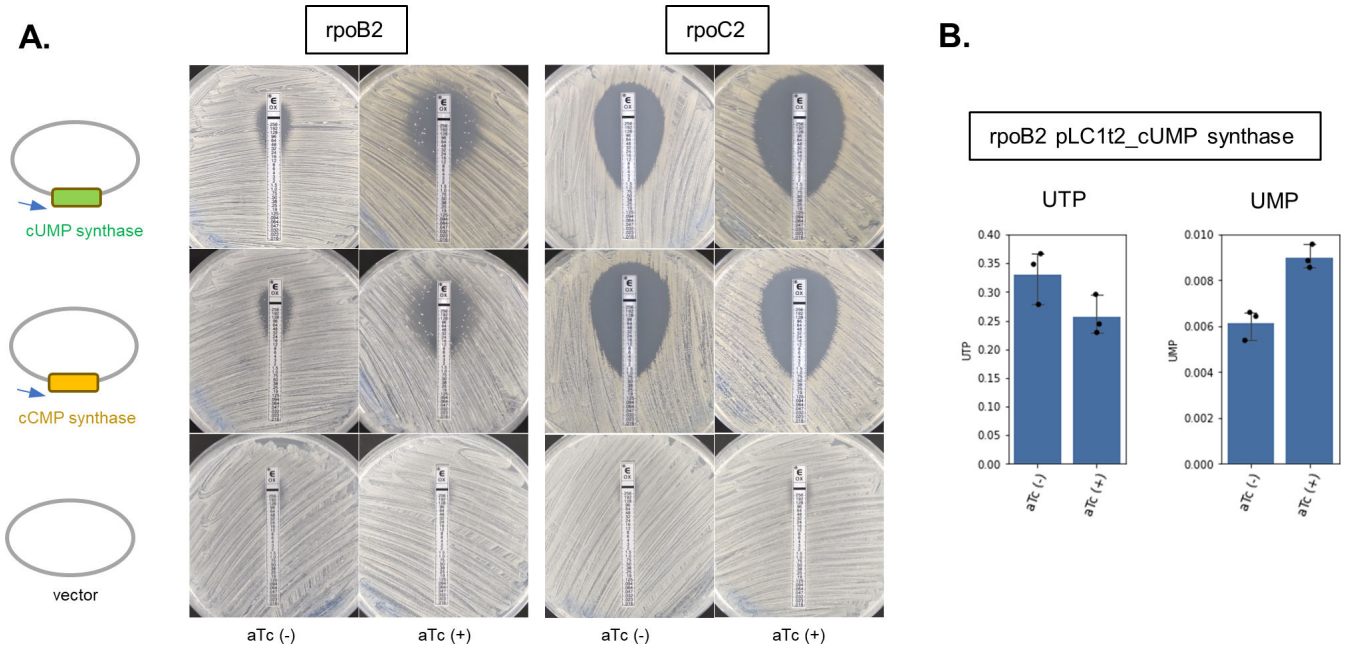

FIG 7 Altered oxacillin susceptibility by cUMP/cCMP gene expressions in JMUB217-derived *rpoBC* mutants. (A) Oxacillin susceptibility of cUMP/cCMP gene-expressing *rpoB2* and *rpoC2* mutants tested by E-test. Oxacillin susceptibility of *S. aureus* JMUB217-22 (*rpoB2*) and JMUB217-24 (*rpoC2*) carrying an aTc-inducible pLC1t2 plasmid containing JMUB217-derived cUMP and JMUB4998-derived cCMP synthase genes, respectively, was measured by oxacillin E-test. The concentration of aTc used for the induction was 50 ng/mL. (B) Relative abundances of intracellular UTP and UMP of *S. aureus* JMUB217-22 (*rpoB2*) harboring pLC1t2_cUMP synthase in the presence/absence of inducer, 50 ng/mL aTc. Data represent means with standard error from three independent experiments.

and food (8–15). Mutations in RNAP gene *rpoB* have been proposed as one of the key chromosomal mutations that contributed to the uniformly high β-lactam-resistant phenotype of OS-MRSA (49). Comparative genomics has revealed that the OS-MRSA JH1 strain acquired three to six mutations, including RpoB$^{D471Y,\ A473S,\ A477S,\ and\ E478D}$, during the course of antibiotic treatment, and the resulting mutant derivative JH2 was rendered oxacillin-, vancomycin-, and rifampicin-resistant (40, 50). Another comparative genome analysis of 15 isolates retrieved from a persistent *S. aureus* infection also identified *rpoB* mutations as genetic determinants responsible for reduced staphylococcal susceptibility to rifampicin and oxacillin (41).

Mutations in *rpoB* are known to confer rifampicin resistance because β subunit of RNAP is the target of rifampicin (34). In addition to rifampicin, different *rpoB* and *rpoC* mutations have been reported to affect the susceptibility of *S. aureus* toward various other antibiotics, such as β-lactams, vancomycin, teicoplanin, linezolid, and daptomycin (21, 22, 25, 36–39, 51–53). *rpoB* mutations, N967I and R644H, caused phenotypic conversion of heterogenous-to-homogeneous and heterogeneous-to-Eagle-type β-lactam resistance, respectively (21). Another *rpoB* mutation, H481Y, was found to induce vancomycin resistance and promote heterogeneous vancomycin-intermediate *S. aureus* (hVISA)-to-VISA conversion (51, 54). Moreover, *rpoBC* mutations have been reported to be accompanied by other phenotypic changes such as prolonged doubling time, decrease in autolysis, and increased linezolid susceptibility, while associated with increased resistance to teicoplanin, vancomycin, and daptomycin (21, 51, 52, 54).

rpoBC-mutated strains included in this study showed reduced susceptibility to oxacillin and other β-lactam antibiotics, such as cefoxitin and imipenem. However, RNAP mutations did not render these strains resistant toward other cell wall synthesis inhibitors (vancomycin, teicoplanin, and fosfomycin) or rifampicin. Considering the distinct antibiotic susceptibility profiles displayed in these JMUB217-derived mutants, *rpoB* mutations carried in our studied strains are proposed to be associated with

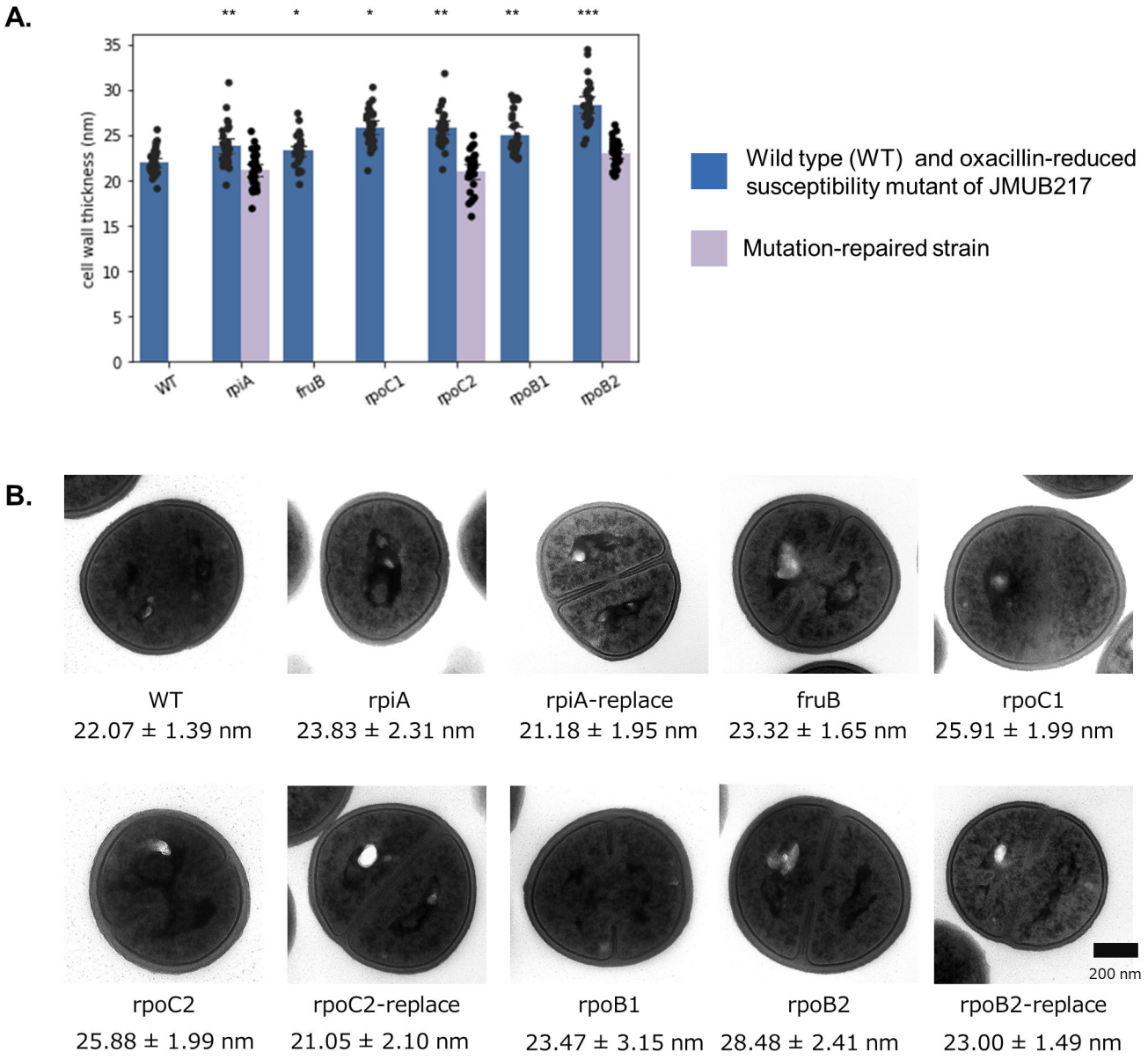

FIG 8 Cell wall thickness of JMUB217-derived mutants. (A) Cell wall thicknesses of 30 cells from each JMUB217-derived mutants with reduced oxacillin susceptibility and the mutation-repaired strains were measured by transmission electron microscopy. Mean values of cell wall thicknesses for JMUB217-derived mutants were compared with that of the wild-type via Student's *t*-test. *$P < 0.05$, **$P < 0.01$, and ***$P < 0.001$. (B) Transmission electron micrographs of representative JMUB217-derived mutants. Magnification, ×30,000.

β-lactam resistance, while other gene mutations and/or different genomic backgrounds of MRSA might be the factor(s) regulating their glycopeptide susceptibility.

Although the association between mutated RNAP genes and reduced oxacillin susceptibility is well-demonstrated, the sequential events succeeding RNAP mutations that led to homogeneous high-level β-lactam resistance are not fully understood. Here, we unraveled the fundamental molecular mechanism linking RNAP gene mutation and staphylococcal β-lactam resistance through CE-TOF-MS-based metabolomics analysis.

Mutations in RNAP genes broadly affect the metabolic states of bacteria in adaptation to a variety of selection pressures, including antibiotics (8, 55–58), high temperature (59), starvation (60), and radiation (61). However, the *rpoBC* mutation-mediated metabolic alterations may differ between organisms. *Escherichia coli* frequently acquired mutations in the *rpoBC* genes in adaptation to glycerol minimum media (60). One of the mutants,

which carries a 27-bp deletion in *rpoC,* demonstrated improved growth in glycerol media through reorganization of the metabolic network. This included an increase in redox cofactors NADH/NADPH and a decrease in most metabolites (tri/di-ribonucleotides) (62), which is in opposition to the case of OS-MRSA. In *E. coli*, the mutations in genes encoding RNAP are suggested to mimic the effect of a stringent response effector (p)ppGpp (60), which can directly bind to β′- and ω-subunits of RNAP, whereas in *Bacillus subtilis*, (p)ppGpp-mediated regulation is indirect and relies on cellular GDP/GTP ratio (63, 64), whereby depletion of cellular GTP is the trigger of the (p)ppGpp-mediated stringent response in Gram-positive bacteria (65). The reduction of oxacillin susceptibility in the *rpoBC* mutants might therefore not be directly related to (p)ppGpp-mediated response because our metabolome analysis shows an increase in intracellular GTP and undetectable (p)ppGpp level in the *rpoBC* mutants. On the other hand, rifampicin-treated *M. tuberculosis* showed dysregulation of nucleotide synthesis. Downregulation of purines (GTP, XTP, dATP, and dADP) and pyrimidines (CDP, dCDP, dCTP, and dTMP), as well as upregulation of ADP, cAMP, UTP, UDP, dUMP, and TDP nucleotides, were detected in *M. tuberculosis* following rifampicin exposure (66). The reported metabolomes were distinct from our *rpoBC*-mutated OS-MRSA strains, which showed an intracellular accumulation of ribonucleoside-di/triphosphate. *M. tuberculosis* with the *rpoB* mutation also showed a reduction in coenzyme A, while CoA was accumulated in our studied *rpoBC* mutants.

Nonetheless, certain *rpoB*-associated metabolic alterations persist across bacterial strains/genera. Exposure of *M. tuberculosis* to rifampicin is accompanied by degradation of mRNA (66). Likewise, *rpoBC* mutations were proposed in this study to reduce the general transcription activity of OS-MRSA as implicated by decreased total RNA levels. Apart from that, in concordance with the excessive amount of NTPs detected in our *rpoBC*-mutated OS-MRSA mutants, a laboratory-derived Mu3-6R strain carrying $RpoB^{R512P}$ showed intracellular ribonucleotide accumulation in addition to slow growth phenotype and vancomycin resistance (39). Extracellular bases and nucleosides, such as inosine, uridine, guanine, cytidine, and guanosine, were also commonly found to be increased in *Streptomyces coelicolor* M1146 with *rpoB* mutation (67). Last but not least, increased peptidoglycan precursors and thickened cell walls were shown in the *rpoBC* mutants included in this study. It is interesting to note that these features were shared with *M. tuberculosis* carrying *rpoB* mutation in which alterations in metabolites associated with the maintenance of cell wall biosynthesis/cell wall remodeling and a paralleled change in cell wall structure were observable (68, 69).

Our previous study identified 141 mutations in 46 genes and 8 intergenic regions as potential genetic determinants of reduced oxacillin susceptibility (8). In this study, *rpiA* and *fruB* mutants (two other frequently mutated genes in OS-MRSA-derived mutants with reduced oxacillin susceptibility), in addition to *rpoBC* mutants, were analyzed. Our metabolomics analysis revealed that both *rpiA* and *fruB* mutations cause loss of function as implicated by the accumulation of substrates in the mutants. However, there is yet insubstantial experimental proof to support the deduction of the mechanism of reduced oxacillin susceptibility mediated through *rpiA* or *fruB* mutations. Further study is needed to warrant a more comprehensive understanding of the role(s) of *rpiA* and *fruB* in the acquisition of reduced oxacillin susceptibility in OS-MRSA.

This study revealed a novel mechanism for the acquisition of reduced β-lactam susceptibility in *S. aureus*. We proposed that mutations in *rpoB* and *rpoC* lead to the dysregulation of RNAP transcription activity and subsequent intracellular accumulation of ribonucleotides. This results in cell wall thickening and reduced β-lactam susceptibility in OS-MRSA. Mutations impacting nucleotide metabolisms [such as purine/pyrimidine metabolism, (p)ppGpp synthesis, and c-di-AMP signal] are often identified after cellular exposure to β-lactams, indicating their importance to β-lactam susceptibility. However, more studies are necessary to establish the intricate connection between chromosomal gene mutations and β-lactam susceptibility in *S. aureus*.

MATERIALS AND METHODS

Bacterial strains and growth conditions

The bacterial strains used in this study included one OS-MRSA parent strain JMUB217 (SCC*mec* type V, ST772, *blaI*-1 and -2 positive) and six of its representative derivative mutants with reduced susceptibility to oxacillin: JMUB217-7 (RpiA^{A64E}), JMUB217-13 (FruB^{A211E}), JMUB217-23 (RpoB^{H929P}), JMUB217-22 (RpoB^{Q645H}), JMUB217-19 (RpoC^{G950R}), and JMUB217-24 (RpoC^{G498D}) (8). All *S. aureus* strains were cultivated either in tryptic soy broth/agar (TSB/TSA; Becton Dickinson) or Mueller–Hinton broth/agar (MHB/MHA; Becton Dickinson) and incubated overnight at 37°C with constant agitation at 200 rpm if grown in broth. For plasmid propagation, *Escherichia coli* BL21 and DH5α strains were grown in Luria–Bertani (LB; Becton Dickinson) medium and incubated overnight at 37°C. To maintain plasmid pIMAY, 10 µg/mL chloramphenicol was added to the growth medium. All strains were stored at −80°C in 40% glycerol (Wako Pure Chemical, Japan) for preservation.

Antibiotic susceptibility tests

The minimum inhibitory concentrations of oxacillin, cefoxitin, imipenem, vancomycin, teicoplanin, sulfamethoxazole/trimethoprim, fosfomycin, and rifampicin were determined using E-test method following the guidelines of the Clinical Laboratory Standard Institute (70).

Construction of mutation-repaired strains

pIMAY-mediated allelic exchange (71) was conducted to construct mutation-repaired strains of JMUB217-7 (*rpiA*), JMUB217-22, (*rpoB*), and JMUB217-24 (*rpoC*) to confirm the effects of these mutations on oxacillin susceptibility. Briefly, native *rpiA*, *rpoB*, and *rpoC* of about 2 kbp each were amplified by pIMAY-N43rpiA-F/-R, pIMAY-N52rpoB-F/-R, and pIMAY-N75rpoC-F/R, respectively, using PRIME STAR MAX (TaKaRa, Japan) from template DNA of wild-type JMUB217. Using NEBuilder HiFi DNA Assembly (New England BioLabs, Inc.), each of the amplified fragment (native *rpiA*, *rpoB*, and *rpoC*) was cloned onto the pIMAY vector backbone linearized by PCR using a primer set of pIMAY-DW-F/pIMAY-DW-R2. The primers used for the construction of plasmids are listed in Fig. S1 and Table S2. The assembled plasmid DNAs were transformed into chemically competent *E. coli* DH5α, and the transformed cells were plated on LB agar with 10 µg/mL chloramphenicol. All three plasmids extracted from DH5α were then transformed into *E. coli* BL21 to improve their transformation efficiency into *S. aureus*. The plasmids extracted from BL21 were electroporated into the corresponding *S. aureus* mutants JMUB217-7, -22, or -24, and the cells were cultured at 30°C on TSA containing 10 µg/mL chloramphenicol. Single crossover was performed by growing overnight culture of transformants on TSA with 10 µg/mL chloramphenicol at 37°C. Then, double crossover was performed by incubating the single crossover mutants on TSA at 30°C. The double crossover event was confirmed by PCR and Sanger sequencing.

Construction of cCMP and cUMP overexpression mutants

S. aureus JMUB217-22 (*rpoB*) and JMUB217-24 (*rpoC*) carrying aTc-inducible pLC1t2 plasmid cloned with JMUB217-derived cUMP and JMUB4998-derived cCMP synthase genes were constructed. At first, the SoxR terminator derived from pBTBX-2 was integrated into the pLC1 plasmid to decrease the downstream expression of an aTc-regulated inducible gene. SoxR terminator of 180 bp and a pLC1 backbone of 6 kbp were amplified by pBTBX2-F3/-R4 and pBTBX2-F3-pLC1dnF/pBTBX2-R4-pLC1upR, respectively, using PRIME STAR MAX and template DNA of pBTBX-2 (72) and pLC1 (73) plasmids. The PCR-amplified fragments were assembled by NEBuilder HiFi DNA Assembly generating pLC1t2. Next, cUMP and cCMP genes were, respectively, amplified by pLC1t2-N9_cUMPsyt-F1/R1 and pLC1t2-JMUB4998_cCMPsyt-F1/R1 from template

DNA of wild-type OS-MRSA JMUB217 and JMUB4998 (8). The cUMP and cCMP gene fragments were then cloned with NEBuilder HiFi DNA Assembly onto the pLC1t2 vector backbone linearized by PCR using a primer set of pLC1t2-F-1/R-1. The assembled plasmid DNAs were transformed into competent *E. coli* DH5α cells, and then the extracted plasmids were subsequently transformed into *E. coli* BL21. The plasmids extracted from BL21 were electroporated into the corresponding *S. aureus* mutants JMUB217-22 or -24, and the resultant transformants were grown on TSA supplemented with 10 µg/mL chloramphenicol at 37°C. The expression of cUMP and cCMP genes were induced by a final concentration of 50 ng/mL aTC added to MHB/MHA media containing 2 µg/mL chloramphenicol.

Metabolite extraction

Overnight cultures of parent *S. aureus* JMUB217 and mutant strains were diluted to OD_{600} = 1.0 with MHB. One milliliter of the culture was added to 50 mL of MHB, and the bacteria were incubated at 37°C with shaking until OD_{600} = 0.5. Then, the cultures were quickly chilled on ice for 15 min. Forty milliliters of the culture was transferred into a 50 mL tube, and the cells were collected by centrifugation at 5,800 × *g* for 5 min at 4°C. Pelleted cells were washed twice with Milli-Q water before being treated with 1,600 µL of methanol and ultrasonicated for 30 s to dissolve the pellet. The cell extract was subsequently treated with 1,100 µL of Milli-Q water containing internal standards [H3304-1002, Human Metabolome Technologies, Inc. (HMT), Tsuruoka, Yamagata, Japan] and left at rest for another 30 s. Cell extract containing spiked in internal standards was centrifuged at 2,300 × *g* for 5 min at 4°C, and 1,400 µL of supernatant was collected. The recovered supernatant was then centrifugally filtered through a Millipore 5 kDa cutoff filter (UltrafreeMC-PLHCC, HMT) at 9,100 × *g* for 120 min at 4°C to remove macromolecules, and the filtrate was finally centrifugally concentrated and resuspended in 50 µL of Milli-Q water for metabolome analysis at HMT. Three biological replicates were prepared for each OS-MRSA-derived mutant and parent strain.

Metabolome analysis

Metabolome analysis was conducted by Basic Scan package of HMT using capillary electrophoresis time-of-flight mass spectrometry as described previously (45, 74). Briefly, CE-TOF-MS analysis was carried out using an Agilent CE capillary electrophoresis system equipped with an Agilent 6210 time-of-flight mass spectrometer (Agilent Technologies, Inc., Santa Clara, CA, USA). The systems were controlled by Agilent G2201AA ChemStation software version B.03.01 (Agilent Technologies, Inc.). Sample separations were carried out using fused silica capillary (50 µm i.d. × 80 cm total length) with commercial electrophoresis buffer (H3301-1001 and I3302-1023 for cation and anion analyses, respectively, HMT) as electrolyte. The spectrometer was scanned from *m/z* 50–1,000, and peaks were extracted using MasterHands, an automatic integration software (Keio University, Tsuruoka, Yamagata, Japan), to obtain peak information, which includes *m/z*, peak area, and migration time (MT) (75). Signal peaks corresponding to isotopomers, adduct ions, and other product ions of known metabolites were excluded. The remaining peaks were annotated according to the HMT metabolite database based on their *m/z* values with the MT determined by CE-TOF-MS. Areas of the annotated peaks were then normalized against internal standard levels and sample amounts in order to obtain the relative levels of each metabolite. Primary 110 metabolites were absolutely quantified based on one-point calibrations using their respective standard compounds. Hierarchical cluster analysis and principal component analysis (76) were performed by HMT's proprietary MATLAB and R program, respectively. Detected metabolites were plotted on metabolic pathway maps using VANTED software (77). Network analysis was performed by Miru (Kajeka, UK) using Pearson correlation matrix with correlation coefficients of 0.85.

Quantification of total RNA

Overnight cultures of the parent OS-MRSA JMUB217 and its derivative mutants with reduced oxacillin susceptibility/mutation-repair grown, respectively, in 1 mL of MHB (Becton Dickinson) were diluted to 1:100 in 10 mL of MHB and incubated at 37°C with constant agitation until OD_{600} of 0.5. The cells were harvested by centrifugation at 15,000 rpm for 1 min, resuspended in 600 µL of $T_{10}E_{10}$ buffer, pH 8.0 (10 mM Tris-HCl 8.0, 10 mM EDTA, pH 8.0), and lysed with a combination of 2 µL of 2 mg/mL lysostaphin (Sigma-Aldrich, USA) and 2 µL of achromopeptidase (FUJIFILM Wako Pure Chemicals, Japan) at 37°C for 5 min. To the lysed cells, 700 µL of acidic phenol saturated with 20 mM sodium acetate (NaOAc) and 60 µL of 3 M NaOAc (pH 4.8) were added. Consequently, total RNA was extracted using the phenol/chloroform method. The extracted RNA was treated with DNase I (Nippon Gene, CO., LTD.) and purified by acidic phenol/ethanol precipitation. The purified total RNA was finally dissolved in an appropriate volume of DEPC water, and the concentration was determined by NanoDrop (Thermo Fisher Scientific). Three biological replicates were prepared for each OS-MRSA-derived mutant, mutation-repaired strain, and parent strain.

qRT-PCR

The extracted total RNA (500 ng per sample) was reverse transcribed into complementary DNA (cDNA) by PrimeScript 1st strand cDNA synthesis Kit (TaKaRa Bio, Japan). qRT-PCR was performed using TB Green Premix Ex Taq II (TaKaRa Bio, Japan). Primer sets used for the amplification of *mecA*, *purF,* and *guaA* are listed in Fig. S1 and Table S2. *rho* gene was used as the reference gene for normalization during gene expression analysis. The thermal cycling conditions included initial denaturation at 95°C for 30 s followed by 40 cycles of 95°C for 5 s and 60°C for 30 s. Three biological replicates were prepared for each strain.

Transmission electron microscopy

To confirm the effects of metabolic alterations on peptidoglycan biosynthesis, cell wall thickness of parent OS-MRSA JMUB217 and its derivative mutants with reduced oxacillin susceptibility/mutation-repair was determined using the transmission electron microscope. Briefly, overnight cultures of the strains grown in MHB were passaged into fresh prewarmed MHB and incubated at 37°C with constant agitation until OD_{600} of 1.0. The cells were harvested by centrifugation at 10,000 rpm for 1 min at 4°C and resuspended with cold 0.1 M phosphate buffer, pH 7.4. Fixation, embedding, and staining of the samples were carried out following the methods described previously (37, 78, 79). The samples were visualized with transmission electron microscopy (Hitachi H-7600, Japan), and cell wall thicknesses were measured at nearly equatorial cut surfaces.

ACKNOWLEDGMENTS

This work was supported by the JSPS KAKENHI (Grant Nos. 19K08960 and 22K19386 to S.W., 20F20104 and 21K19488 to L.C.), JSPS Invitational Fellowship for Research in Japan (Long-term L21543 to S.W. and C.A.N.), Takeda Science Foundation (to S.W.), and the Japan Agency for Medical Research and Development (Grant No. JP21fk0108497 to S.W., JP21fk0108496 and JP21wm0325022 to K.K., JP22ae0121045, JP21gm1610002, and JP20fk0108134 to L.C.). The funders had no role in the study design, data collection and analysis, the decision to publish, and manuscript preparation.

S.W., C.A.N., and L.C. designed the study, analyzed the data, and wrote the manuscript. K.T., X.-E.T., Y.A., and R.T. contributed to the acquisition, analysis, and interpretation of data, and assisted in the preparation of the manuscript. All other authors contributed to data collection and interpretation and critically revised the manuscript. All authors approved the final version of the manuscript and agreed on all aspects of the work in ensuring that questions related to the accuracy or integrity of any part of the work are appropriately investigated and resolved.

The authors declare that this research was conducted in the absence of any commercial or financial relationships that could be construed as a potential conflict of interest.

AUTHOR AFFILIATIONS

[1]Division of Bacteriology, Department of Infection and Immunity, Jichi Medical University, Tochigi, Japan
[2]Department of Biotechnology, School of Biological Sciences, Federal University of Technology Owerri Nigeria, Owerri, Nigeria
[3]School of Medicine, Jichi Medical University, Tochigi, Japan
[4]Research Center for Drug and Vaccine Development, National Institute of Infectious Diseases, Tokyo, Japan

AUTHOR ORCIDs

Shinya Watanabe http://orcid.org/0000-0003-3932-8575
Xin-Ee Tan http://orcid.org/0000-0001-7847-2583
Kotaro Kiga http://orcid.org/0000-0002-0248-6951

FUNDING

Funder	Grant(s)	Author(s)
MEXT | Japan Society for the Promotion of Science (JSPS)	19K08960	Shinya Watanabe
MEXT | Japan Society for the Promotion of Science (JSPS)	22K19386	Shinya Watanabe
MEXT | Japan Society for the Promotion of Science (JSPS)	20F20104	Longzhu Cui
MEXT | Japan Society for the Promotion of Science (JSPS)	21K19488	Longzhu Cui
MEXT | Japan Society for the Promotion of Science (JSPS)	L21543	Shinya Watanabe Chijioke A. Nsofor
Takeda Science Foundation (TSF)		Shinya Watanabe
Japan Agency for Medical Research and Development (AMED)	JP21fk0108497	Shinya Watanabe
Japan Agency for Medical Research and Development (AMED)	JP21fk0108496	Kotaro Kiga
Japan Agency for Medical Research and Development (AMED)	JP21wm0325022	Kotaro Kiga
Japan Agency for Medical Research and Development (AMED)	JP22ae0121045	Longzhu Cui
Japan Agency for Medical Research and Development (AMED)	JP21gm1610002	Longzhu Cui
Japan Agency for Medical Research and Development (AMED)	JP20fk0108134	Longzhu Cui

AUTHOR CONTRIBUTIONS

Shinya Watanabe, Writing – review and editing, Conceptualization, Data curation, Formal analysis, Funding acquisition, Investigation, Methodology, Project administration, Supervision, Validation, Visualization, Writing – review and editing | Chijioke A. Nsofor, Writing – review and editing, Conceptualization, Formal analysis, Funding acquisition, Visualization, Writing – review and editing | Xin-Ee Tan, Funding acquisition, Writing – review and editing | Yoshifumi Aiba, Funding acquisition, Writing – review and editing |

Remi Takenouchi, Funding acquisition, Writing – review and editing | Kotaro Kiga, Formal analysis, Writing – review and editing | Teppei Sasahara, Resources, Writing – review and editing | Kazuhiko Miyanaga, Writing – review and editing | Srivani Veeranarayanan, Writing – review and editing | Yuzuki Shimamori, Writing – review and editing | Adeline Yeo Syin Lian, Writing – review and editing | Thuy Minh Nguyen, Writing – review and editing | Huong Minh Nguyen, Writing – review and editing | Ola Alessa, Writing – review and editing | Geoffrey Peterkins Kumwenda, Writing – review and editing | Sarangi Jayathilake, Writing – review and editing | Jastin Edrian Cocuangco Revilleza, Writing – review and editing | Priyanka Baranwal, Writing – review and editing | Yutaro Nishikawa, Writing – review and editing | Feng-Yu Li, Writing – review and editing | Tomofumi Kawaguchi, Writing – review and editing | Sowmiya Sankaranarayanan, Writing – review and editing | Mahmoud Arbaah, Writing – review and editing | Yuancheng Zhang, Writing – review and editing | Maniruzzaman , Writing – review and editing | Yi Liu, Writing – review and editing | Hossain Sarah, Writing – review and editing | Junjie Li, Writing – review and editing | Takashi Sugano, Writing – review and editing | Thi My Duyen Ho, Writing – review and editing | Anujin Batbold, Writing – review and editing | Tergel Nayanjin, Writing – review and editing, Formal analysis, Writing – review and editing | Longzhu Cui, Writing – review and editing, Formal analysis, Writing – review and editing.

ADDITIONAL FILES

The following material is available online.

Supplemental Material

Fig. S1 and Table S2 (mBio00339-24-s0001.docx). Metabolic alteration with regard to central metabolomic pathways in JMUB217-derived mutants and primer list.
Table S1 (mBio00339-24-s0002.xlsx). Metabolomics data.

REFERENCES

1. Murray CJL, Ikuta KS, Sharara F, Swetschinski L, Robles Aguilar G, Gray A, Han C, Bisignano C, Rao P, Wool E, et al. 2022. Global burden of bacterial antimicrobial resistance in 2019: a systematic analysis. Lancet 399:629–655. https://doi.org/10.1016/S0140-6736(21)02724-0
2. Hartman BJ, Tomasz A. 1984. Low-affinity penicillin-binding protein associated with beta-lactam resistance in *Staphylococcus aureus*. J Bacteriol 158:513–516. https://doi.org/10.1128/jb.158.2.513-516.1984
3. Utsui Y, Yokota T. 1985. Role of an altered penicillin-binding protein in methicillin- and cephem-resistant *Staphylococcus aureus*. Antimicrob Agents Chemother 28:397–403. https://doi.org/10.1128/AAC.28.3.397
4. Fishovitz J, Hermoso JA, Chang M, Mobashery S. 2014. Penicillin-binding protein 2a of methicillin-resistant *Staphylococcus aureus*. IUBMB Life 66:572–577. https://doi.org/10.1002/iub.1289
5. Foster TJ. 2017. Antibiotic resistance in *Staphylococcus aureus*. Current status and future prospects. FEMS Microbiol Rev 41:430–449. https://doi.org/10.1093/femsre/fux007
6. Llarrull LI, Fisher JF, Mobashery S. 2009. Molecular basis and phenotype of methicillin resistance in *Staphylococcus aureus* and insights into new β-lactams that meet the challenge. Antimicrob Agents Chemother 53:4051–4063. https://doi.org/10.1128/AAC.00084-09
7. Fuda CCS, Fisher JF, Mobashery S. 2005. β-lactam resistance in *Staphylococcus aureus*: the adaptive resistance of a plastic genome. Cell Mol Life Sci 62:2617–2633. https://doi.org/10.1007/s00018-005-5148-6
8. Boonsiri T, Watanabe S, Tan X-E, Thitiananpakorn K, Narimatsu R, Sasaki K, Takenouchi R, Sato'o Y, Aiba Y, Kiga K, Sasahara T, Taki Y, Li F-Y, Zhang Y, Azam AH, Kawaguchi T, Cui L. 2020. Identification and characterization of mutations responsible for the β-lactam resistance in oxacillin-susceptible *mecA* -positive *Staphylococcus aureus*. Sci Rep 10:16907. https://doi.org/10.1038/s41598-020-73796-5
9. Hiramatsu K, Kihara H, Yokota T. 1992. Analysis of borderline-resistant strains of methicillin-resistant *Staphylococcus aureus* using polymerase chain reaction. Microbiol Immunol 36:445–453. https://doi.org/10.1111/j.1348-0421.1992.tb02043.x
10. Saeed K, Ahmad N, Dryden M, Cortes N, Marsh P, Sitjar A, Wyllie S, Bourne S, Hemming J, Jeppesen C, Green S. 2014. Oxacillin-susceptible methicillin-resistant *Staphylococcus aureus* (OS-MRSA), a hidden resistant mechanism among clinically significant isolates in the Wessex region/UK. Infection 42:843–847. https://doi.org/10.1007/s15010-014-0641-1
11. Andrade-Figueiredo M, Leal-Balbino TC. 2016. Clonal diversity and epidemiological characteristics of *Staphylococcus aureus*: high prevalence of oxacillin-susceptible *mecA*-positive *Staphylococcus aureus* (OS-MRSA) associated with clinical isolates in Brazil. BMC Microbiol 16:115. https://doi.org/10.1186/s12866-016-0733-4
12. Song Y, Cui L, Lv Y, Li Y, Xue F. 2017. Characterisation of clinical isolates of oxacillin-susceptible *mecA*-positive *Staphylococcus aureus* in China from 2009 to 2014. J Glob Antimicrob Resist 11:1–3. https://doi.org/10.1016/j.jgar.2017.05.009
13. Quijada NM, Hernández M, Oniciuc E-A, Eiros JM, Fernández-Natal I, Wagner M, Rodríguez-Lázaro D. 2019. Oxacillin-susceptible *mecA*-positive *Staphylococcus aureus* associated with processed food in Europe. Food Microbiol 82:107–110. https://doi.org/10.1016/j.fm.2019.01.021
14. Hososaka Y, Hanaki H, Endo H, Suzuki Y, Nagasawa Z, Otsuka Y, Nakae T, Sunakawa K. 2007. Characterization of oxacillin-susceptible *mecA*-positive *Staphylococcus aureus*: a new type of MRSA. J Infect Chemother 13:79–86. https://doi.org/10.1007/s10156-006-0502-7
15. Balslev U, Bremmelgaard A, Svejgaard E, Havstreym J, Westh H. 2005. An outbreak of borderline oxacillin-resistant *Staphylococcus aureus* (BORSA) in a dermatological unit. Microb Drug Resist 11:78–81. https://doi.org/10.1089/mdr.2005.11.78
16. Kishii K, Ito T, Watanabe S, Okuzumi K, Hiramatsu K. 2008. Recurrence of heterogeneous methicillin-resistant *Staphylococcus aureus* (MRSA) among the MRSA clinical isolates in a Japanese university hospital. J Antimicrob Chemother 62:324–328. https://doi.org/10.1093/jac/dkn186

17. Hartman BJ, Tomasz A. 1986. Expression of methicillin resistance in heterogeneous strains of *Staphylococcus aureus*. Antimicrob Agents Chemother 29:85–92. https://doi.org/10.1128/AAC.29.1.85
18. Mwangi MM, Kim C, Chung M, Tsai J, Vijayadamodar G, Benitez M, Jarvie TP, Du L, Tomasz A. 2013. Whole-genome sequencing reveals a link between β-lactam resistance and synthetases of the alarmone (p)ppGpp in *Staphylococcus aureus*. Microb Drug Resist 19:153–159. https://doi.org/10.1089/mdr.2013.0053
19. Tomasz A, Nachman S, Leaf H. 1991. Stable classes of phenotypic expression in methicillin-resistant clinical isolates of staphylococci. Antimicrob Agents Chemother 35:124–129. https://doi.org/10.1128/AAC.35.1.124
20. Skinner S, Murray M, Walus T, Karlowsky JA. 2009. Failure of cloxacillin in treatment of a patient with borderline oxacillin-resistant *Staphylococcus aureus* endocarditis. J Clin Microbiol 47:859–861. https://doi.org/10.1128/JCM.00571-08
21. Aiba Y, Katayama Y, Hishinuma T, Murakami-Kuroda H, Cui L, Hiramatsu K. 2013. Mutation of RNA polymerase β-subunit gene promotes heterogeneous-to-homogeneous conversion of β-lactam resistance in methicillin-resistant *Staphylococcus aureus*. Antimicrob Agents Chemother 57:4861–4871. https://doi.org/10.1128/AAC.00720-13
22. Matsuo M, Yamamoto N, Hishinuma T, Hiramatsu K. 2019. Identification of a novel gene associated with high-level β-lactam resistance in heterogeneous vancomycin-intermediate *Staphylococcus aureus* strain Mu3 and methicillin-resistant *S. aureus* strain N315. Antimicrob Agents Chemother 63:e00712-18. https://doi.org/10.1128/AAC.00712-18
23. Chung M, Kim CK, Conceição T, Aires-De-Sousa M, De Lencastre H, Tomasz A. 2016. Heterogeneous oxacillin-resistant phenotypes and production of PBP2A by oxacillin-susceptible/*mecA*-positive MRSA strains from Africa. J Antimicrob Chemother 71:2804–2809. https://doi.org/10.1093/jac/dkw209
24. Gratani FL, Horvatek P, Geiger T, Borisova M, Mayer C, Grin I, Wagner S, Steinchen W, Bange G, Velic A, Maček B, Wolz C. 2018. Regulation of the opposing (p)ppGpp synthetase and hydrolase activities in a bifunctional RelA/SpoT homologue from *Staphylococcus aureus*. PLoS Genet 14:e1007514. https://doi.org/10.1371/journal.pgen.1007514
25. Panchal VV, Griffiths C, Mosaei H, Bilyk B, Sutton JAF, Carnell OT, Hornby DP, Green J, Hobbs JK, Kelley WL, Zenkin N, Foster SJ. 2020. Evolving MRSA: high-level β-lactam resistance in *Staphylococcus aureus* is associated with RNA polymerase alterations and fine tuning of gene expression. PLoS Pathog 16:e1008672. https://doi.org/10.1371/journal.ppat.1008672
26. Pozzi C, Waters EM, Rudkin JK, Schaeffer CR, Lohan AJ, Tong P, Loftus BJ, Pier GB, Fey PD, Massey RC, O'Gara JP. 2012. Methicillin resistance alters the biofilm phenotype and attenuates virulence in *Staphylococcus aureus* device-associated infections. PLoS Pathog 8:e1002626. https://doi.org/10.1371/journal.ppat.1002626
27. Dordel J, Kim C, Chung M, Pardos de la Gándara M, Holden MTJ, Parkhill J, de Lencastre H, Bentley SD, Tomasz A. 2014. Novel determinants of antibiotic resistance: identification of mutated loci in highly methicillin-resistant subpopulations of methicillin-resistant *Staphylococcus aureus*. mBio 5:e01000. https://doi.org/10.1128/mBio.01000-13
28. Berger-Bächi B, Strässle A, Gustafson JE, Kayser FH. 1992. Mapping and characterization of multiple chromosomal factors involved in methicillin resistance in *Staphylococcus aureus*. Antimicrob Agents Chemother 36:1367–1373. https://doi.org/10.1128/AAC.36.7.1367
29. Berger-Bächi B. 1983. Insertional inactivation of staphylococcal methicillin resistance by Tn551. J Bacteriol 154:479–487. https://doi.org/10.1128/jb.154.1.479-487.1983
30. Barba-Aliaga M, Alepuz P, Pérez-Ortín JE. 2021. Eukaryotic RNA polymerases: the many ways to transcribe a gene. Front Mol Biosci 8:663209. https://doi.org/10.3389/fmolb.2021.663209
31. Weiss A, Shaw LN. 2015. Small things considered: the small accessory subunits of RNA polymerase in Gram-positive bacteria. FEMS Microbiol Rev 39:541–554. https://doi.org/10.1093/femsre/fuv005
32. Klein-Marcuschamer D, Santos CNS, Yu H, Stephanopoulos G. 2009. Mutagenesis of the bacterial RNA polymerase alpha subunit for improvement of complex phenotypes. Appl Environ Microbiol 75:2705–2711. https://doi.org/10.1128/AEM.01888-08
33. Sydow JF, Cramer P. 2009. RNA polymerase fidelity and transcriptional proofreading. Curr Opin Struct Biol 19:732–739. https://doi.org/10.1016/j.sbi.2009.10.009
34. Campbell EA, Korzheva N, Mustaev A, Murakami K, Nair S, Goldfarb A, Darst SA. 2001. Structural mechanism for rifampicin inhibition of bacterial RNA polymerase. Cell 104:901–912. https://doi.org/10.1016/s0092-8674(01)00286-0
35. Campodónico VL, Rifat D, Chuang Y-M, Ioerger TR, Karakousis PC. 2018. Altered *Mycobacterium tuberculosis* cell wall metabolism and physiology associated with RpoB mutation H526D. Front Microbiol 9:494. https://doi.org/10.3389/fmicb.2018.00494
36. Matsuo M, Hishinuma T, Katayama Y, Hiramatsu K. 2015. A mutation of RNA polymerase β′ subunit (RpoC) converts heterogeneously vancomycin-intermediate *Staphylococcus aureus* (hVISA) into "Slow VISA". Antimicrob Agents Chemother 59:4215–4225. https://doi.org/10.1128/AAC.00135-15
37. Hanaki H, Kuwahara-Arai K, Boyle-Vavra S, Daum RS, Labischinski H, Hiramatsu K. 1998. Activated cell-wall synthesis is associated with vancomycin resistance in methicillin-resistant *Staphylococcus aureus* clinical strains Mu3 and Mu50. J Antimicrob Chemother 42:199–209. https://doi.org/10.1093/jac/42.2.199
38. Yu R, Dale SE, Yamamura D, Stankus V, Lee C. 2012. Daptomycin-nonsusceptible, vancomycin-intermediate, methicillin-resistant *Staphylococcus aureus* endocarditis. Can J Infect Dis Med Microbiol 23:e48–e50. https://doi.org/10.1155/2012/138470
39. Katayama Y, Azechi T, Miyazaki M, Takata T, Sekine M, Matsui H, Hanaki H, Yahara K, Sasano H, Asakura K, Takaku T, Ochiai T, Komatsu N, Chambers HF. 2017. Prevalence of slow-growth vancomycin nonsusceptibility in methicillin-resistant *Staphylococcus aureus*. Antimicrob Agents Chemother 61:e00452-17. https://doi.org/10.1128/AAC.00452-17
40. Mwangi MM, Wu SW, Zhou Y, Sieradzki K, de Lencastre H, Richardson P, Bruce D, Rubin E, Myers E, Siggia ED, Tomasz A. 2007. Tracking the *in vivo* evolution of multidrug resistance in *Staphylococcus aureus* by whole-genome sequencing. Proc Natl Acad Sci U S A 104:9451–9456. https://doi.org/10.1073/pnas.0609839104
41. Klein S, Morath B, Weitz D, Schweizer PA, Sähr A, Heeg K, Boutin S, Nurjadi D. 2022. Comparative genomic reveals clonal heterogeneity in persistent *Staphylococcus aureus* infection. Front Cell Infect Microbiol 12:817841. https://doi.org/10.3389/fcimb.2022.817841
42. Morrow TO, Harmon SA. 1979. Genetic analysis of *Staphylococcus aureus* RNA polymerase mutants. J Bacteriol 137:374–383. https://doi.org/10.1128/jb.137.1.374-383.1979
43. Aubry-Damon H, Soussy C-J, Courvalin P. 1998. Characterization of mutations in the*rpoB* gene that confer rifampin resistance in*Staphylococcus aureus*. Antimicrob Agents Chemother (Bethesda) 42:2590–2594. https://doi.org/10.1128/AAC.42.10.2590
44. Mitsuishi Y, Taguchi K, Kawatani Y, Shibata T, Nukiwa T, Aburatani H, Yamamoto M, Motohashi H. 2012. Nrf2 redirects glucose and glutamine into anabolic pathways in metabolic reprogramming. Cancer Cell 22:66–79. https://doi.org/10.1016/j.ccr.2012.05.016
45. Ohashi Y, Hirayama A, Ishikawa T, Nakamura S, Shimizu K, Ueno Y, Tomita M, Soga T. 2008. Depiction of metabolome changes in histidine-starved *Escherichia coli* by CE-TOFMS. Mol Biosyst 4:135–147. https://doi.org/10.1039/b714176a
46. Tal N, Morehouse BR, Millman A, Stokar-Avihail A, Avraham C, Fedorenko T, Yirmiya E, Herbst E, Brandis A, Mehlman T, Oppenheimer-Shaanan Y, Keszei AFA, Shao S, Amitai G, Kranzusch PJ, Sorek R. 2021. Cyclic CMP and cyclic UMP mediate bacterial immunity against phages. Cell 184:5728–5739. https://doi.org/10.1016/j.cell.2021.09.031
47. Reeves RE, Warren LG, Hsu DS. 1966. 1-Phosphofructokinase from an anaerobe. J Biol Chem 241:1257–1261. https://doi.org/10.1016/S0021-9258(18)96768-2
48. Zhang R guang, Andersson CE, Savchenko A, Skarina T, Evdokimova E, Beasley S, Arrowsmith CH, Edwards AM, Joachimiak A, Mowbray SL. 2003. Structure of *Escherichia coli* ribose-5-phosphate isomerase: a ubiquitous enzyme of the pentose phosphate pathway and the calvin cycle. Structure 11:31–42. https://doi.org/10.1016/s0969--2126(02)00933-4
49. Hiramatsu K, Ito T, Tsubakishita S, Sasaki T, Takeuchi F, Morimoto Y, Katayama Y, Matsuo M, Kuwahara-Arai K, Hishinuma T, Baba T. 2013.

Genomic basis for methicillin resistance in *Staphylococcus aureus*. Infect Chemother 45:117–136. https://doi.org/10.3947/ic.2013.45.2.117
50. Sieradzki K, Leski T, Dick J, Borio L, Tomasz A. 2003. Evolution of a vancomycin-intermediate *Staphylococcus aureus* strain *in vivo*: multiple changes in the antibiotic resistance phenotypes of a single lineage of methicillin-resistant *S. aureus* under the impact of antibiotics administered for chemotherapy. J Clin Microbiol 41:1687–1693. https://doi.org/10.1128/JCM.41.4.1687-1693.2003
51. Katayama Y, Murakami-Kuroda H, Cui L, Hiramatsu K. 2009. Selection of heterogeneous vancomycin-intermediate *Staphylococcus aureus* by imipenem. Antimicrob Agents Chemother 53:3190–3196. https://doi.org/10.1128/AAC.00834-08
52. Cui L, Isii T, Fukuda M, Ochiai T, Neoh H-M, Camargo ILB da C, Watanabe Y, Shoji M, Hishinuma T, Hiramatsu K. 2010. An RpoB mutation confers dual heteroresistance to daptomycin and vancomycin in *Staphylococcus aureus*. Antimicrob Agents Chemother 54:5222–5233. https://doi.org/10.1128/AAC.00437-10
53. Matsuo M, Hishinuma T, Katayama Y, Cui L, Kapi M, Hiramatsu K. 2011. Mutation of RNA polymerase β subunit (*rpoB*) promotes hVISA-to-VISA phenotypic conversion of strain Mu3. Antimicrob Agents Chemother 55:4188–4195. https://doi.org/10.1128/AAC.00398-11
54. Watanabe Y, Cui L, Katayama Y, Kozue K, Hiramatsu K. 2011. Impact of *rpoB* mutations on reduced vancomycin susceptibility in *Staphylococcus aureus*. J Clin Microbiol 49:2680–2684. https://doi.org/10.1128/JCM.02144-10
55. Severinov K, Soushko M, Goldfarb A, Nikiforov V. 1993. Rifampicin region revisited. New rifampicin-resistant and streptolydigin-resistant mutants in the beta subunit of *Escherichia coli* RNA polymerase. J Biol Chem 268:14820–14825. https://doi.org/10.1016/S0021-9258(18)82407-3
56. Reynolds MG. 2000. Compensatory evolution in rifampin-resistant *Escherichia coli*. Genetics 156:1471–1481. https://doi.org/10.1093/genetics/156.4.1471
57. Duchi D, Mazumder A, Malinen AM, Ebright RH, Kapanidis AN. 2018. The RNA polymerase clamp interconverts dynamically among three states and is stabilized in a partly closed state by ppGpp. Nucleic Acids Res 46:7284–7295. https://doi.org/10.1093/nar/gky482
58. Degen D, Feng Y, Zhang Y, Ebright KY, Ebright YW, Gigliotti M, Vahedian-Movahed H, Mandal S, Talaue M, Connell N, Arnold E, Fenical W, Ebright RH. 2014. Transcription inhibition by the depsipeptide antibiotic salinamide A. Elife 3:e02451. https://doi.org/10.7554/eLife.02451
59. Tenaillon O, Rodríguez-Verdugo A, Gaut RL, McDonald P, Bennett AF, Long AD, Gaut BS. 2012. The molecular diversity of adaptive convergence. Science 335:457–461. https://doi.org/10.1126/science.1212986
60. Conrad TM, Frazier M, Joyce AR, Cho B-K, Knight EM, Lewis NE, Landick R, Palsson BØ. 2010. RNA polymerase mutants found through adaptive evolution reprogram *Escherichia coli* for optimal growth in minimal media. Proc Natl Acad Sci U S A 107:20500–20505. https://doi.org/10.1073/pnas.0911253107
61. Bruckbauer ST, Trimarco JD, Martin J, Bushnell B, Senn KA, Schackwitz W, Lipzen A, Blow M, Wood EA, Culberson WS, Pennacchio C, Cox MM. 2019. Experimental evolution of extreme resistance to ionizing radiation in *Escherichia coli* after 50 cycles of selection. J Bacteriol 201:e00784-18. https://doi.org/10.1128/JB.00784-18
62. Cheng K-K, Lee B-S, Masuda T, Ito T, Ikeda K, Hirayama A, Deng L, Dong J, Shimizu K, Soga T, Tomita M, Palsson BO, Robert M. 2014. Global metabolic network reorganization by adaptive mutations allows fast growth of *Escherichia coli* on glycerol. Nat Commun 5:3233. https://doi.org/10.1038/ncomms4233
63. Hauryliuk V, Atkinson GC, Murakami KS, Tenson T, Gerdes K. 2015. Recent functional insights into the role of (p)ppGpp in bacterial physiology. Nat Rev Microbiol 13:298–309. https://doi.org/10.1038/nrmicro3448
64. Krásný L, Gourse RL. 2004. An alternative strategy for bacterial ribosome synthesis: *Bacillus subtilis* rRNA transcription regulation. EMBO J 23:4473–4483. https://doi.org/10.1038/sj.emboj.7600423
65. Geiger T, Wolz C. 2014. Intersection of the stringent response and the CodY regulon in low GC Gram-positive bacteria. Int J Med Microbiol 304:150–155. https://doi.org/10.1016/j.ijmm.2013.11.013
66. Yelamanchi SD, Mishra A, Behra SK, Karthikkeyan G, Keshava Prasad TS, Surolia A. 2022. Rifampicin-mediated metabolic changes in *Mycobacterium tuberculosis*. Metabolites 12:493. https://doi.org/10.3390/metabo12060493
67. Nitta K, Breitling R, Takano E, Putri SP, Fukusaki E. 2021. Investigation of the effects of actinorhodin biosynthetic gene cluster expression and a *rpoB* point mutation on the metabolome of *Streptomyces coelicolor* M1146. J Biosci Bioeng 131:525–536. https://doi.org/10.1016/j.jbiosc.2021.01.002
68. Loots DT. 2016. New insights into the survival mechanisms of rifampicin-resistant *Mycobacterium tuberculosis*. J Antimicrob Chemother 71:655–660. https://doi.org/10.1093/jac/dkv406
69. Rêgo AM, Alves da Silva D, Ferreira NV, de Pina LC, Evaristo JAM, Caprini Evaristo GP, Nogueira FCS, Ochs SM, Amaral JJ, Ferreira RBR, Antunes LCM. 2021. Metabolic profiles of multidrug resistant and extensively drug resistant *Mycobacterium tuberculosis* unveiled by metabolomics. Tuberculosis (Edinb) 126:102043. https://doi.org/10.1016/j.tube.2020.102043
70. Clinical and Laboratory Standards Institute. 2013. M100-S23. Performance standards for antimicrobial susceptibility testing; twenty-third informational supplement. CLSI, Wayne, PA, USA.
71. Monk IR, Shah IM, Xu M, Tan M-W, Foster TJ. 2012. Transforming the untransformable: application of direct transformation to manipulate genetically *Staphylococcus aureus* and *Staphylococcus epidermidis*. mBio 3:e00277-11. https://doi.org/10.1128/mBio.00277-11
72. Prior JE, Lynch MD, Gill RT. 2010. Broad-host-range vectors for protein expression across gram negative hosts. Biotechnol Bioeng 106:326–332. https://doi.org/10.1002/bit.22695
73. Cui L, Neoh H, Iwamoto A, Hiramatsu K. 2012. Coordinated phenotype switching with large-scale chromosome flip-flop inversion observed in bacteria. Proc Natl Acad Sci U S A 109:E1647–E1656. https://doi.org/10.1073/pnas.1204307109
74. Ooga T, Sato H, Nagashima A, Sasaki K, Tomita M, Soga T, Ohashi Y. 2011. Metabolomic anatomy of an animal model revealing homeostatic imbalances in dyslipidaemia. Mol Biosyst 7:1217–1223. https://doi.org/10.1039/c0mb00141d
75. Sugimoto M, Wong DT, Hirayama A, Soga T, Tomita M. 2010. Capillary electrophoresis mass spectrometry-based saliva metabolomics identified oral, breast and pancreatic cancer-specific profiles. Metabolomics 6:78–95. https://doi.org/10.1007/s11306-009-0178-y
76. Yamamoto H, Fujimori T, Sato H, Ishikawa G, Kami K, Ohashi Y. 2014. Statistical hypothesis testing of factor loading in principal component analysis and its application to metabolite set enrichment analysis. BMC Bioinformatics 15:51. https://doi.org/10.1186/1471-2105-15-51
77. Junker BH, Klukas C, Schreiber F. 2006. VANTED: a system for advanced data analysis and visualization in the context of biological networks. BMC Bioinformatics 7:109. https://doi.org/10.1186/1471-2105-7-109
78. Cui L, Murakami H, Kuwahara-Arai K, Hanaki H, Hiramatsu K. 2000. Contribution of a thickened cell wall and its glutamine nonamidated component to the vancomycin resistance expressed by *Staphylococcus aureus* Mu50. Antimicrob Agents Chemother 44:2276–2285. https://doi.org/10.1128/AAC.44.9.2276-2285.2000
79. Thitiananpakorn K, Aiba Y, Tan X-E, Watanabe S, Kiga K, Sato'o Y, Boonsiri T, Li F-Y, Sasahara T, Taki Y, Azam AH, Zhang Y, Cui L. 2020. Association of *mprF* mutations with cross-resistance to daptomycin and vancomycin in methicillin-resistant *Staphylococcus aureus* (MRSA). Sci Rep 10:16107. https://doi.org/10.1038/s41598-020-73108-x